

UNIVERSITY OF OKLAHOMA

GRADUATE COLLEGE

AN INVESTIGATION OF TRICUSPID VALVE LEAFLET DECELLULARIZATION AND  
EFFECTS ON LEAFLET BIOMECHANICS AND COLLAGEN ARCHITECTURE

A THESIS

SUBMITTED TO THE GRADUATE FACULTY

in partial fulfillment of the requirements for the

Degree of

MASTER OF SCIENCE

By

CATHERINE ANN VOPAT

Norman, Oklahoma

2022

AN INVESTIGATION OF TRICUSPID VALVE LEAFLET DECELLULARIZATION AND  
EFFECTS ON LEAFLET BIOMECHANICS AND COLLAGEN ARCHITECTURE

A THESIS APPROVED FOR THE  
STEPHENSON SCHOOL OF BIOMEDICAL ENGINEERING

BY THE COMMITTEE CONSISTING OF

Dr. Chung-Hao Lee, Chair

Dr. Handan Acar

Dr. Sarah Breen

© Copyright by CATHERINE ANN VOPAT 2022  
All Rights Reserved.

## **Acknowledgements**

First, I would like to say thank you to my advisor, Dr. Lee, for mentoring me over the last two years and helping me to achieve my goals despite the campus lockdown that occurred at the beginning of my master's degree. It is through his mentorship that I have been able to finish my thesis on time despite the initial setback, and I am grateful for the guidance he has provided me. I would also like to thank my committee members Dr. Acar and Dr. Breen for their commitment to helping me improve my thesis and develop as a critical thinker. Dr. Acar's courses have been some of my favorite classes at OU, and Dr. Breen's positive energy was much appreciated during my thesis defense. I would also like to specially thank Colton for his mentorship and support during my time in BBDL, Elizabeth and Caylin for making 6 am experiments really fun, and all of the other talented researchers that I have worked with. Finally, I wouldn't be where I am today without the support and love of my parents, Tommy, and Steven.

# Abstract

The Tricuspid Heart Valve is composed of three leaflets: the anterior leaflet, posterior leaflet, and septal leaflet. The function of this valve is to open during diastole to allow blood to flow from the atrium to the ventricle, then close during systole to prevent backwards flow of blood, called regurgitation. Valve regurgitation can decrease the effectiveness of the heartbeat and can lead to death over time. Two common heart valve replacements are mechanical heart valves and xenografts. These options have both shown clinical success, however no replacement currently meets the criteria for hemocompatibility, immunological tolerance, and the potential to grow and remodel itself. The decellularized tissue-engineered heart valve (TEHV) may be the key to achieving all of these goals. Decellularization has the potential to remove any immunogenic markers from the tissue while maintaining the complex microstructure that is vital for proper cell differentiation and remodeling. In this study, an H&E staining procedure was optimized for further use in the lab. Nine decellularization procedures with different exposure times to detergent and enzyme solutions were compared to find the optimal procedure. We found that 24-hour exposure to detergent and 12-hour exposure to enzymes was the optimal decellularization procedure for all three leaflets. This optimized decellularization procedure was then used in a biaxial mechanical and collagen microstructural analysis study to determine if the biaxial mechanical characteristics and collagen fiber architecture change as a result of the decellularization treatment. After statistical analysis of several parameters, we found that there were no statistically significant changes from the pre-treatment values to the post-treatment values due to decellularization reagent exposure. These results provide strong evidence that the chosen decellularization procedure is effective at decellularizing the tissue while maintaining the microstructure architecture and mechanical properties of the native leaflet.

# Table of Contents

|  |    |
|--|----|
| <i>Abstract</i> .....  | v  |
| <i>Table of Contents</i> .....   | vi |
| <i>Chapter 1 - Introduction</i> .....  | 1  |
| 1.1 Motivation .....   | 1  |
| 1.2 Objective and Scope .....  | 2  |
| <i>Chapter 2 - Background Information</i> .....  | 4  |
| 2.1 Anatomy and Function of the Tricuspid Heart Valve .....  | 4  |
| 2.2 Tricuspid Valve Pathology and Treatment Options .....  | 6  |
| 2.3 Tissue-Engineered Heart Valves .....   | 7  |
| <i>Chapter 3 - Histology Optimization</i> .....  | 10 |
| 3.1 Methods.....   | 11 |
| 3.2 Results .....  | 14 |
| 3.3 Discussion .....   | 18 |
| <i>Chapter 4 - Decellularization</i> .....   | 19 |
| 4.1 Methods.....   | 19 |
| 4.2 Results- TVSL .....  | 22 |
| 4.3 Results- TVAL.....   | 27 |
| 4.4 Results- TVPL .....  | 28 |
| 4.5 Discussion .....   | 29 |
| <i>Chapter 5 - Analysis of Mechanical Characteristics and Collagen Alignment of Decellularized Tissues</i> ..... | 30 |
| 5.1 Methods.....   | 33 |
| 5.2 Results- Biaxial Testing .....   | 35 |
| 5.3 Results- pSFDI Analysis.....   | 45 |
| 5.4 Discussion .....   | 63 |
| <i>Chapter 6 Conclusions</i> .....   | 65 |
| 6.1 Conclusions and Future Work.....   | 65 |

# List of Figures

|   |    |
|---|----|
| <b>Figure 2-1.</b> The Tricuspid Heart Valve. Image adapted from StatCardiologist.com .....   | 4  |
| <b>Figure 2-2.</b> Heart Anatomy, including the valves and direction of blood flow. Image modified from cardiologyassociatesofmichigan.com <sup>1</sup> .....   | 5  |
| <b>Figure 3-1.</b> 10X magnification of TVPL stained with H&E. Samples A and B were stained with a progressive procedure. Samples C and D were stained with a regressive procedure. Collagen is stained pink, nuclei are stained purple. .... | 15 |
| <b>Figure 3-2.</b> 10X magnification of TVAL stained with H&E. Samples A and B were stained with a progressive procedure. Samples C and D were stained with a regressive procedure. Collagen is stained pink, nuclei are stained purple. .... | 16 |
| <b>Figure 3-3.</b> 10X magnification of TVSL stained with H&E. Samples A and B were stained with a progressive procedure. Samples C and D were stained with a regressive procedure. Collagen is stained pink, nuclei are stained purple. .... | 17 |
| <b>Figure 4-1.</b> TVSL sectioned into 9 circumferentially oriented strips.....   | 19 |
| <b>Figure 4-2.</b> Steps of the decellularization procedure .....   | 21 |
| <b>Figure 4-3.</b> 10X magnification of H&E-stained tissues. Collagen is stained pink and nuclei are stained purple.....  | 22 |
| <b>Figure 4-4.</b> 10X magnification of Alcian Blue-stained tissues. GAGs are stained blue and nuclei are stained purple.....   | 23 |
| <b>Figure 4-5.</b> 4X magnification of Sirius Red-stained tissues. Collagen is stained dark pink. ....  | 24 |
| <b>Figure 4-6.</b> 4X magnification of Trichrome-stained tissues. Collagen is stained blue.....   | 25 |
| <b>Figure 4-7.</b> 10X magnification of Pentachrome-stained tissues. Nuclei and elastin are stained black. Collagen is stained yellow. ....   | 26 |

|  |    |
|--|----|
| <b>Figure 4-8.</b> 10X magnification of H&E-stained tissues. Collagen is stained pink and nuclei are stained purple.....   | 27 |
| <b>Figure 4-9.</b> 10X magnification of H&E-stained tissues. Collagen is stained pink and nuclei are stained purple.....   | 28 |
| <b>Figure 5-1.</b> Representation of $\theta_{\text{Fiber}}$ and DOA parameters.....   | 31 |
| <b>Figure 5-2.</b> a) Schematic of system setup. b) Depiction of $\theta_{\text{Polarizer}}$ and $\theta_{\text{Fiber}}$ including bimodal intensity peak. (Image from Jett et al. 2021 <sup>34</sup> ) .....  | 32 |
| <b>Figure 5-3.</b> Summary of the biaxial/pSFDI, decellularization, biaxial/pSFDI pipeline.....  | 34 |
| <b>Figure 5-4.</b> Membrane tension–stretch curve with high tension moduli and low tension moduli fitted to both the circumferential curve and the radial curve.....   | 35 |
| <b>Figure 5-5.</b> Circumferential low-tension modulus for control and decellularized treatment groups. Pre-treatment values are compared to post-treatment values with a paired $t$ test. Statistical significance is indicated with $*$ = $p < 0.05$ , and $**$ = $p < 0.005$ .....          | 36 |
| <b>Figure 5-6.</b> Circumferential low-tension modulus post-treatment values from the control group are compared to the post-treatment values from the decellularized group with a paired $t$ test. Statistical significance is indicated with $*$ = $p < 0.05$ , and $**$ = $p < 0.005$ ..... | 37 |
| <b>Figure 5-7.</b> Radial low-tension modulus for control and decellularized treatment groups. Pre-treatment values are compared to post-treatment values with a paired $t$ test. Statistical significance is indicated with $*$ = $p < 0.05$ , and $**$ = $p < 0.005$ .....                   | 39 |
| <b>Figure 5-8.</b> Radial low-tension modulus post-treatment values from the control group are compared to the post-treatment values from the decellularized group with a paired $t$ test. Statistical significance is indicated with $*$ = $p < 0.05$ , and $**$ = $p < 0.005$ .....          | 40 |



**Figure 5-9.** Circumferential high-tension modulus for control and decellularized treatment groups. Pre-treatment values are compared to post-treatment values with a paired *t* test. Statistical significance is indicated with \* =  $p < 0.05$  , and \*\* =  $p < 0.005$ .....42

**Figure 5-10.** Circumferential high-tension modulus post-treatment values from the control group are compared to the post-treatment values from the decellularized group with a paired *t* test. Statistical significance is indicated with \* =  $p < 0.05$  , and \*\* =  $p < 0.005$ .....43

**Figure 5-11.** Radial high-tension modulus for control and decellularized treatment groups. Pre-treatment values are compared to post-treatment values with a paired *t* test. Statistical significance is indicated with \* =  $p < 0.05$  , and \*\* =  $p < 0.005$ .....45

**Figure 5-12.** Radial high-tension modulus post-treatment values from the control group are compared to the post-treatment values from the decellularized group with a paired *t* test. Statistical significance is indicated with \* =  $p < 0.05$  , and \*\* =  $p < 0.005$ .....46

**Figure 5-13.** Peak stretch values for each loading protocol before treatment and after treatment in the circumferential direction. Statistical significance is indicated with \* =  $p < 0.05$  , and \*\* =  $p < 0.005$ .....48

**Figure 5-14.** Circumferential peak stretch post-treatment values from the control group are compared to the post-treatment values from the decellularized group with a paired *t* test. Statistical significance is indicated with \* =  $p < 0.05$  , and \*\* =  $p < 0.005$ .....49

**Figure 5-15.** Peak stretch values for each loading protocol before treatment and after treatment in the radial direction. Statistical significance is indicated with \* =  $p < 0.05$  , and \*\* =  $p < 0.005$ .  
.....51

**Figure 5-16.** Radial peak stretch post-treatment values from the control group are compared to the post-treatment values from the decellularized group with a paired *t* test. Statistical significance is indicated with \* =  $p < 0.05$  , and \*\* =  $p < 0.005$ .....52

**Figure 5-17.**  $\theta_{\text{Fiber}}$  values for each loading protocol before treatment and after treatment. Statistical significance is indicated with \* =  $p < 0.05$  , and \*\* =  $p < 0.005$ .....55

**Figure 5-18.**  $\theta_{\text{Fiber}}$  post-treatment values from the control group are compared to the post-treatment values from the decellularized group with a paired *t* test. Statistical significance is indicated with \* =  $p < 0.05$  , and \*\* =  $p < 0.005$ .....56

**Figure 5-19.** DOA values for each loading protocol before treatment and after treatment. Statistical significance is indicated with \* =  $p < 0.05$  , and \*\* =  $p < 0.005$ .....58

**Figure 5-20.** DOA post-treatment values from the control group are compared to the post-treatment values from the decellularized group with a paired *t* test. Statistical significance is indicated with \* =  $p < 0.05$  , and \*\* =  $p < 0.005$ .....59

**Figure 5-21.** Colormap of leaflet before treatment and after treatment under four different loading ratios. White lines represent the average  $\theta_{\text{Fiber}}$  angle of collagen fibers in the area. Colors represent the DOA. ....62

# List of Tables

|  |    |
|--|----|
| <b>Table 3-1.</b> Tissue exposure time in minutes for each reagent of the paraffin infiltration procedure .....  | 11 |
| <b>Table 3-2.</b> Deparaffinization and staining procedures. Procedures A and B are progressive procedures, and Procedures C and D are regressive procedures. .... | 13 |
| <b>Table 4-1.</b> Detergent exposure time (hours) and enzyme exposure time (hours) for each tissue sample.....   | 20 |
| <b>Table 5-1.</b> Summary of the decellularized group procedure vs. the control group procedure .....  | 34 |
| <b>Table 5-2.</b> Circumferential low-tension modulus values and % change from pre-treatment to post-treatment for the control group.....                          | 38 |
| <b>Table 5-3.</b> Circumferential low-tension modulus values and % change from pre-treatment to post-treatment for the decellularized group.....                   | 38 |
| <b>Table 5-4.</b> Radial low-tension modulus values and % change from pre-treatment to post-treatment for the control group.....                                   | 41 |
| <b>Table 5-5.</b> Radial low-tension modulus values and % change from pre-treatment to post-treatment for the decellularized group.....                            | 41 |
| <b>Table 5-6.</b> Circumferential high-tension modulus values and % change from pre-treatment to post-treatment for the control group.....                         | 44 |
| <b>Table 5-7.</b> Circumferential high-tension modulus values and % change from pre-treatment to post-treatment for the decellularized group.....                  | 44 |
| <b>Table 5-8.</b> Radial high-tension modulus values and % change from pre-treatment to post-treatment for the control group.....                                  | 47 |

|  |    |
|--|----|
| <b>Table 5-9.</b> Radial high-tension modulus values and % change from pre-treatment to post-treatment for the decellularized group.....   | 47 |
| <b>Table 5-10.</b> Circumferential peak stretch values and % change from pre-treatment to post-treatment for the control group.....        | 50 |
| <b>Table 5-11.</b> Circumferential peak stretch values and % change from pre-treatment to post-treatment for the decellularized group..... | 50 |
| <b>Table 5-12.</b> Radial peak stretch values and % change from pre-treatment to post-treatment for the control group.....                 | 53 |
| <b>Table 5-13.</b> Radial peak stretch values and % change from pre-treatment to post-treatment for the decellularized group. ....         | 53 |
| <b>Table 5-14.</b> <i>P</i> -value results from one-way MANOVA repeated for each loading protocol.....                                     | 54 |
| <b>Table 5-15.</b> $\theta_{\text{Fiber}}$ values and % change from pre-treatment to post-treatment for the control group.....             | 57 |
| <b>Table 5-16.</b> $\theta_{\text{Fiber}}$ values and % change from pre-treatment to post-treatment for the decellularized group. ....     | 57 |
| <b>Table 5-17.</b> DOA values and % change from pre-treatment to post-treatment for the control group.....                                 | 60 |
| <b>Table 5-18.</b> DOA values and % change from pre-treatment to post-treatment for the decellularized group. ....                         | 60 |
| <b>Table 5-19.</b> <i>P</i> -value results from one-way MANOVA repeated for each loading protocol.....                                     | 61 |

# Chapter 1 - Introduction

The right atrioventricular heart valve, also known as the tricuspid valve, is located at the top of the right ventricle and serves as a gateway between the right atrium and right ventricle. It is composed of three collagenous leaflets which open toward the ventricle as blood rushes from the atrium to the ventricle during diastole. During systole, the right ventricle contracts to move blood through the pulmonary valve and into the pulmonary artery. The tricuspid valve closes during this contraction, preventing backflow of blood into the atrium. This backflow of blood is a condition known as heart valve regurgitation, which inhibits the effectiveness of the heartbeat, causing the heart to work harder. If left untreated, tricuspid valve regurgitation can lead to heart failure. The current options for heart valve replacement have many complications. Mechanical valves have poor hemocompatibility which puts the recipient at increased risk of blood clots, and biological replacements such as xenografts and homografts are likely to calcify or degenerate within ten years of implantation. Current valve replacement options do not grow with the body, so pediatric patients require a series of valve donations as their hearts grow.

## 1.1 Motivation

The tissue-engineered heart valve (TEHV) is a replacement option that has the potential for hemocompatibility, immunological compatibility, and the potential to grow and remodel itself. A valve that achieves these criteria could prevent the need for anticoagulants, immunosuppressants, or reoperation. There are two main types of TEHV scaffolds: decellularized tissue and synthetic polymer scaffolding. Decellularized xenograft heart valves maintain the complex microstructure of the native leaflets, which has an important influence on cell differentiation. However, removal of cellular and genetic material by chemical or

mechanical means has the potential to damage the extracellular matrix (ECM). Damage to the ECM has been characterized using histology and microscopy methods; however, there has not been analysis of how the microstructure behaves under pathologic loads post-decellularization. There is a need to characterize the collagen microstructure and quantify collagen alignment before and after decellularization treatment, as well as analyze the biaxial mechanical characteristics of the leaflets pre- and post-treatment.

## 1.2 Objective and Scope

The objective of this thesis is to analyze the effect of the chosen decellularization treatment on the biaxial mechanical characteristics of the tricuspid valve posterior leaflet. The studies performed to achieve this data are as follows:

1. Histology procedure optimization

Several hematoxylin and eosin procedures were compared to achieve optimal images of the decellularized tissues.

2. Decellularization optimization of the three tricuspid valve leaflets

In this study, a tricuspid valve leaflet was sectioned into 9 strips and exposed to a first solution of Triton X-100 and sodium deoxycholate, then a second solution of DNase and RNase. Strips were exposed to the solutions for 0, 12, and 24 hours. This experiment was repeated for the anterior, posterior, and septal leaflets.

3. Biaxial Mechanical characterization and collagen microstructural analysis pre- and post-treatment

In this study, a tricuspid valve posterior leaflet was biaxially tested under pathological loading conditions. The tissue was placed under various forces in the circumferential and radial directions to simulate diseased conditions in vivo. Collagen alignment was

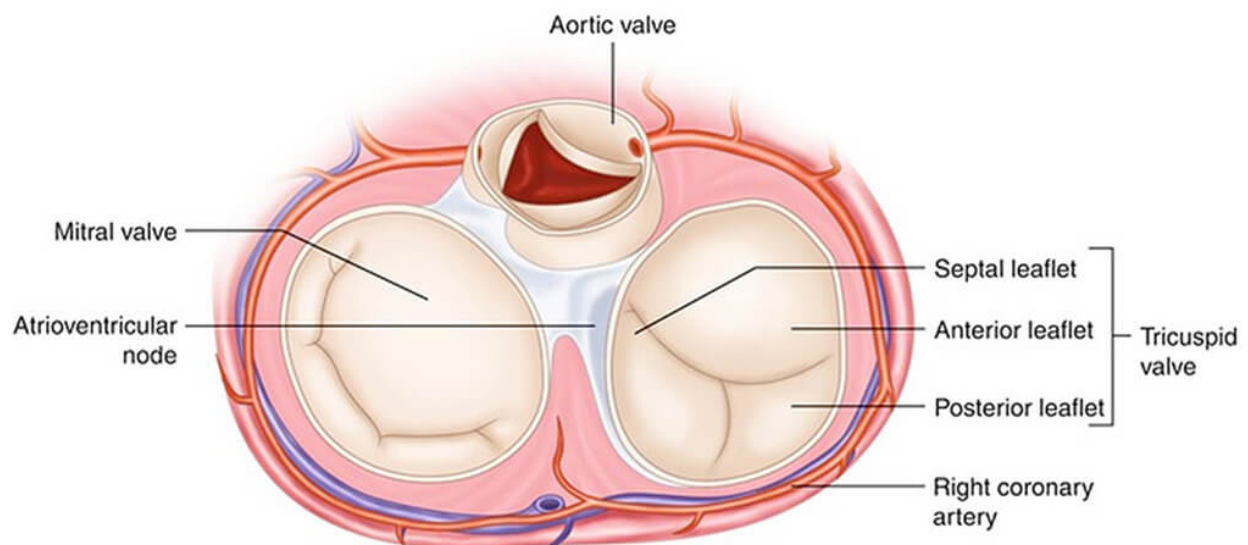
measured under these loading conditions using polarized spatial frequency domain imaging (pSFDI).

Chapter 2 of this thesis provides relevant background information such as the anatomy and function of the tricuspid heart valve, tricuspid valve pathology and current treatment options, and an overview of progress in the field of Tissue-Engineered heart valves. Chapter 3 details the H&E histology procedure comparison to determine the optimal deparaffinization and staining procedures. Chapter 4 presents the methods and results of the decellularization treatment on the three tricuspid leaflets, and Chapter 5 covers the methods and results of the biaxial characterization and pSFDI tests. Finally, Chapter 6 includes a discussion of the key findings from this thesis and future areas of investigation.

# Chapter 2 - Background Information

## 2.1 Anatomy and Function of the Tricuspid Heart Valve

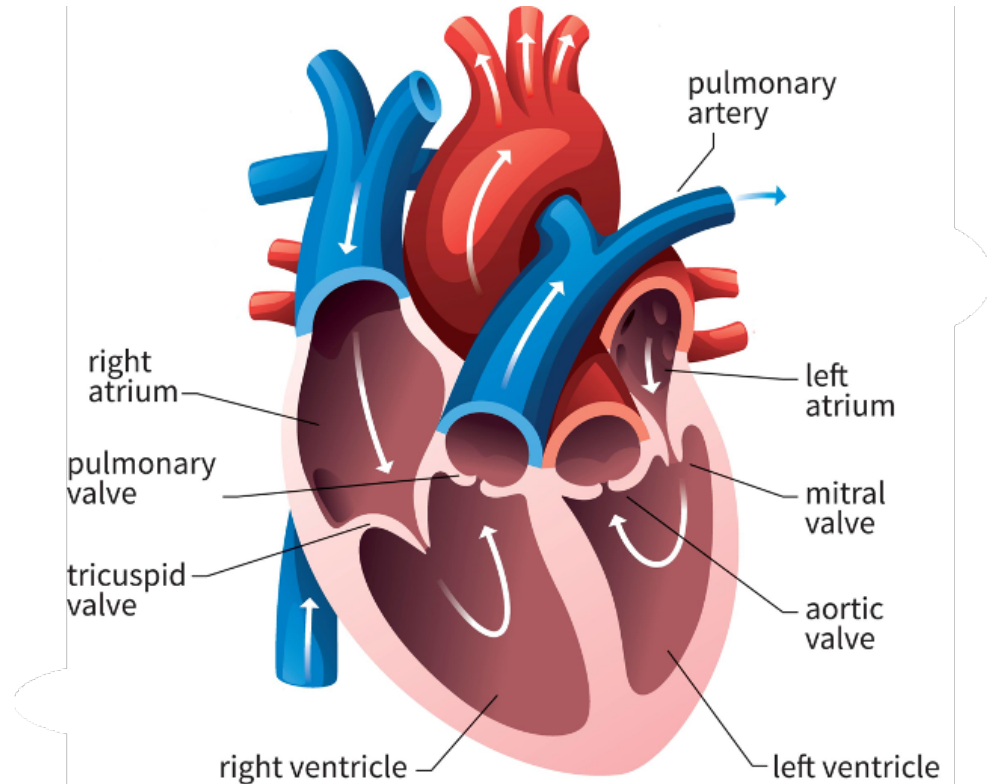
The tricuspid heart valve is located on the right side of the heart, and it is composed of three leaflets: the anterior leaflet, posterior leaflet, and septal leaflet. These leaflets are supported by the annulus, which connects them to the papillary muscles of the heart.



**Figure 2-1.** The Tricuspid Heart Valve. Image adapted from StatCardiologist.com.

The annulus is an elliptical ring of fibrous tissue, and it can change shape as the myocardium contracts during systole. The tricuspid valve's function is to move blood from the right atrium to the right ventricle, and to prevent regurgitation, or backflow, of blood into the atrium. The tricuspid valve leaflets are attached to the ventricular myocardium through collagenous fibers called chordae tendineae, which prevent the leaflets from opening toward the atrium during systole.





**Figure 2-2.** Heart Anatomy, including the valves and direction of blood flow. Image modified from [cardiologyassociatesofmichigan.com](http://cardiologyassociatesofmichigan.com).<sup>1</sup>

The tricuspid valve leaflet microstructure is primarily composed of collagen, elastin, and glycosaminoglycans, and all constituents are distributed heterogeneously. Tricuspid valve leaflets are separated into four distinct layers: the atrialis, spongiosa, fibrosa, and ventricularis. The atrialis is a monolayer of valvular endothelial cells (VECs) and the matrix is primarily composed of elastin.<sup>2</sup> The spongiosa is a layer of primarily glycosaminoglycans and proteoglycans, and is thought to act as lubricant between the atrialis and fibrosa layers.<sup>3</sup> The fibrosa is primarily composed of collagen fibers, and the ventricularis layer is composed of collagen and elastin.

## 2.2 Tricuspid Valve Pathology and Treatment Options

Tricuspid pathology has two classifications: primary pathology, due to an intrinsic valvular condition, and secondary pathology, which occurs as a result of disease elsewhere in the heart<sup>4</sup>. Primary tricuspid valve pathology can be congenital, as in Ebstein's anomaly, a disorder characterized by a fenestrated anterior leaflet and hypoplastic septal and posterior leaflets.<sup>5</sup> Primary pathology can also be acquired through endocarditis, radiation, damage due to cardiac device leads, and trauma, amongst others.<sup>6</sup> Tricuspid valve secondary pathology can result from disease in the left heart valves, myocardium, or pulmonary artery.<sup>6</sup>

One of the most common tricuspid valve pathologies is regurgitation, or the backward leakage of blood into the right atrium. Tricuspid regurgitation has been classified into two categories: functional and non-functional. Functional regurgitation is a direct result of pathology elsewhere in the heart, such as in left heart valve disease, myocardial disease, or pulmonary hypertension. Non-functional tricuspid regurgitation, or primary regurgitation, is due to damage of the tricuspid leaflets, annulus, chordae, or papillary muscles, and is seen less frequently.<sup>7</sup>

Another notable tricuspid pathology is stenosis, or narrowing of the valvular orifice. Rheumatic heart disease is a major cause of tricuspid stenosis, characterized by excessive fibrous thickening and fused valvular commissures.<sup>8</sup> This disease is an autoimmune reaction in response to infection by group A streptococcus, and leads to around 250,000 deaths per year globally.<sup>9</sup> Aside from rheumatic disease, stenosis can be caused by carcinoid tumor lesions, a pathology characterized by stiffened leaflets coated in plaque, obstructive vegetation due to infective endocarditis, congenitally underdeveloped tricuspid valves, or right ventricular tumors.<sup>8</sup>

Severe functional regurgitation is typically treated using surgical methods such as annuloplasty, a procedure designed to reduce annular diameter or reinforce annular geometry, as well as anterior leaflet enlargement, which involves replacement of the autologous anterior leaflet with a larger patch of pericardium. Leaflet stenosis due to primary valvular disease can be treated by replacement of affected area with a pericardial patch,<sup>10</sup> however, in many patients with valvular disease, valve damage is too extensive for surgical repair.<sup>11</sup> This creates the need for cost effective, readily available, and safe valve replacement options.

## 2.3 Tissue-Engineered Heart Valves

The ideal Tissue-Engineered heart valve should provide a scaffold for host cells to proliferate and remodel, integrating the graft into the host anatomy. There are currently two main types of scaffolds under investigation: decellularized tissue and synthetic polymer scaffolds.<sup>12</sup> Synthetic scaffolds do not require human or animal tissue donation and are therefore more readily available, however, a high degree of microstructural anisotropy is necessary to mimic native leaflet biomechanics.<sup>13</sup> Tissue scaffold decellularization preserves the complex network of collagen, elastin, and glycosaminoglycans, which has been shown to positively impact the differentiation of valvular interstitial cells (VICs),<sup>14</sup> a major component of native valve anatomy.

The primary drawback of xenograft scaffolds for Tissue Engineering applications is the potential for host immune response. Galactose- $\alpha$ 1,3-Galactose, also known as  $\alpha$ -Gal or Gal epitope, is a cell membrane antigen that has been identified as a major cause of inflammation and ultimate transplant rejection. It is estimated that up to 1% of human Immunoglobulin G (IgG) antibodies are anti-Gal as a result of constant exposure to  $\alpha$ -Gal+ bacteria in the digestive tract.<sup>15</sup> Host anti-Gal antibodies binding to  $\alpha$ -Gal epitopes upon transplantation activates the complement cascade which can destroy the xenograft in minutes, a condition known as

hyperacute rejection.<sup>16</sup> The depletion or neutralization of anti-Gal antibodies from the host blood stream in combination with immunosuppressive therapy can delay this response, however once the antibodies are replenished, the graft will be rejected immediately.<sup>17</sup> Even if hyperacute rejection can be avoided, acute humoral xenograft rejection (AHXR) can occur days later from a combination of antibody deposition and innate immune cell infiltration.<sup>18</sup> In addition to cell-surface proteins, foreign DNA and RNA have the potential to induce an immune response during xenotransplantation, however it has been shown clinically that small DNA fragments (<300 bp) are not enough to induce an immune response.<sup>19</sup> Removal of cell surface antigens and genetic material through decellularization techniques may be the key to xenotransplantation without the need for host immune suppression.

Xenografts implanted into the human body tend to exhibit one of two possible long-term remodeling responses. The first is characterized by chronic inflammation and fibrous encapsulation, and the second by organized and appropriate tissue remodeling.<sup>20</sup> Chemical crosslinking of collagen fibers within ECM scaffolds has been used as a method to increase durability of implanted tissue scaffolding over time, however this change in tissue topology has been shown to induce a pro-inflammatory phenotype (M1) in local macrophages, leading to chronic inflammation.<sup>21, 22</sup> By contrast, immunomodulatory macrophages (M2) induce proteolytic ECM degradation, which has been shown to release chemotactic signals which recruit multipotential progenitor cells to the scaffold site and trigger differentiation.<sup>23, 24</sup> Because the purpose of the TEHV is to be broken down and remodeled, chemical crosslinking was not employed in this study.

There are many methods of tissue decellularization, including the use of ionic, non-ionic, and zwitter-ionic detergent to lyse cell membranes, enzymes such as nucleases which cleave

genetic material, and mechanical methods such as osmotic shock, pressure gradients, radiation, and many others. In 2017, VeDepo *et al.* reported over the various methods of heart valve decellularization and included the decellularization effectiveness as well as the general effect of the procedure on the ECM. The most promising method was shown to be a combination of Triton X-100 and sodium deoxycholate, which showed complete lack of nuclei, 98% DNA removal, and histological preservation of the ECM.<sup>12</sup> This method, in combination with DNase and RNase treatment to reduce leftover genetic material, may be the key to producing a heart valve ECM scaffold that is hemocompatible, immunologically compatible, and readily remodeled by native host cells.

## Chapter 3 - Histology Optimization

A robust procedure to differentiate between nuclei and other tissue components is necessary to establish the efficacy of the chosen decellularization method. Most tissues appear colorless and possess similar optical densities when studied under a light microscope,<sup>25</sup> so stain is introduced to differentiate between components. Anionic molecules such as nucleic acids are referred to as basophilic, meaning they bind with basic stains. Likewise, cationic molecules such as collagen and cytoplasmic components are acidophilic. Hematoxylin and Eosin staining, or H&E, is the most commonly used staining procedure due to its relatively simple procedure and inexpensive cost.<sup>25</sup> Hematoxylin targets acidic molecules such as nucleic acid, which renders nuclei dark purple when viewed under a microscope. A counterstain of Eosin Y binds to cytoplasm, collagen, and smooth muscle, dyeing the positively charged materials pink.<sup>26</sup>

There are two distinct H&E procedures referred to as progressive and regressive staining. With a progressive stain procedure, tissues are exposed to hematoxylin just long enough to stain anionic nuclei, then washed in water to remove unbound hematoxylin.<sup>26</sup> Regressive staining involves over-staining the tissue with hematoxylin, then removing excess hematoxylin with a differentiator such as acetic acid. This method is ideal for charged slides, which tend to induce background staining of non-nuclear material.<sup>27</sup>

Before tissues can be stained, embedded wax must be removed in a process called deparaffinization. Multiple xylene clearant baths can be used to remove paraffin wax. Xylene is insoluble in water, so excess clearant must be removed from the slide via alcohol baths starting at a concentration of 100% and subsequently decreasing.<sup>26</sup> Then, tissues are hydrated in a water bath before staining with aqueous hematoxylin.

In this study, two deparaffinization protocols were compared with a progressive stain procedure and a regressive stain procedure to determine the optimal combination.

### 3.1 Methods

Each leaflet was sectioned into three circumferential strips, and strips were fixed in 10% neutral buffered formalin for 24 hours. Paraffin infiltration was performed according to the procedure in Table 3-1.

**Table 3-1.** Tissue exposure time for each reagent of the paraffin infiltration procedure.

| <b>Reagent</b> | <b>Time (minutes)</b> |
|----------------|-----------------------|
| 70% Alcohol    | 30                    |
| 95% Alcohol    | 30                    |
| 100% Alcohol   | 30                    |
| 100% Alcohol   | 30                    |
| 100% Alcohol   | 30                    |
| 100% Alcohol   | 60                    |
| Xylene         | 30                    |
| Xylene         | 15                    |
| Xylene         | 15                    |
| Wax            | 30                    |
| Wax            | 60                    |

Tissues were then embedded into paraffin blocks and sectioned into 5-micron ribbons. Paraffin ribbons were placed in a water bath at 37 °C to smooth wrinkles in the section, then sections were floated onto charged glass slides. Two sections were adhered to each slide, and two slides were made for each tissue strip.

Four test groups were implemented to determine the optimal deparaffinization and staining procedure. The test groups were labeled A, B, C, and D, and the procedures are listed in Table 3-2.



**Table 3-2.** Deparaffinization and staining procedures. Procedures A and B are progressive procedures, and Procedures C and D are regressive procedures.

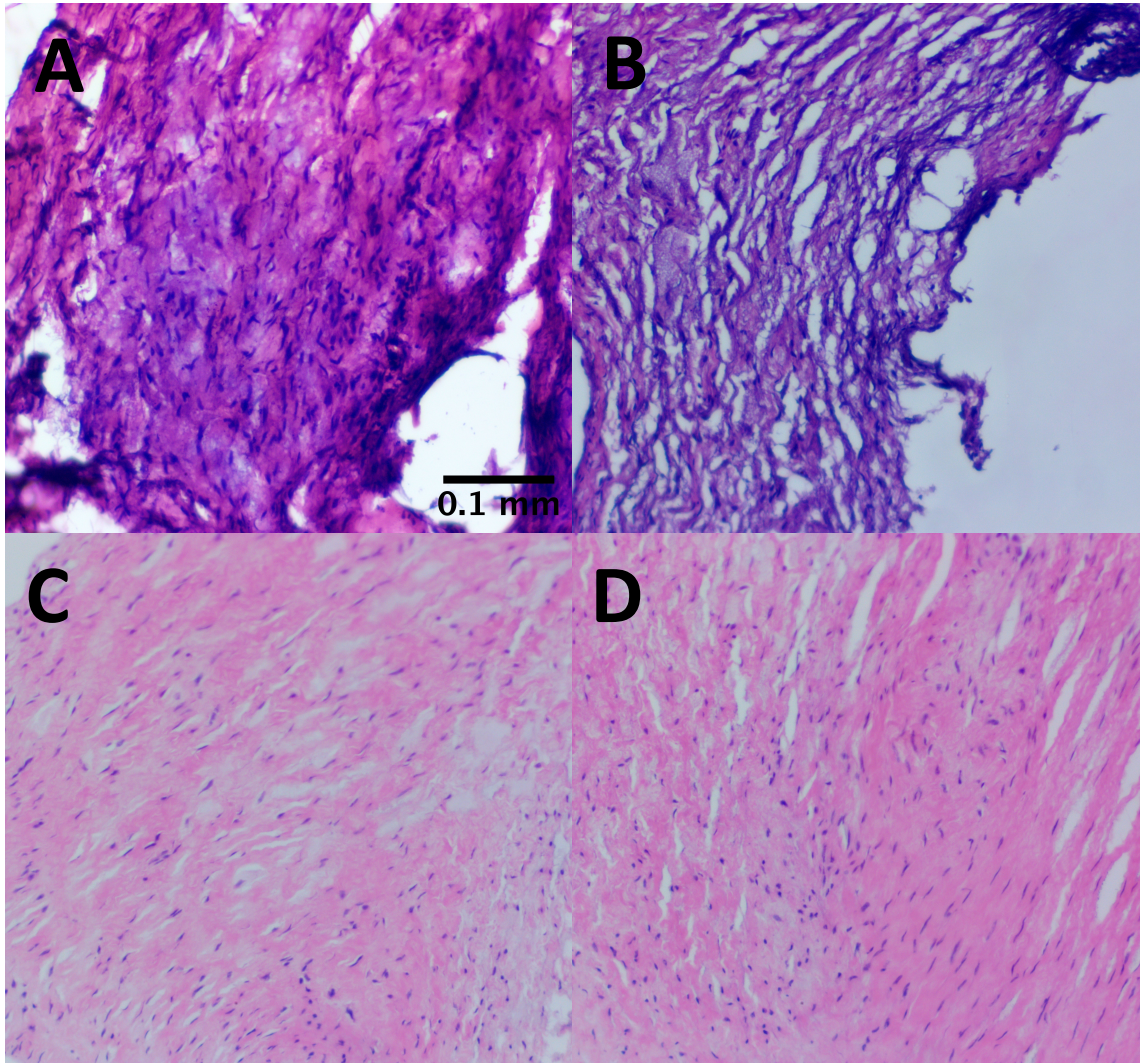
| A        |              | B        |              | C      |              | D      |              |
|----------|--------------|----------|--------------|--------|--------------|--------|--------------|
| 3 mins   | xylene       | 2 mins   | xylene       | 2 mins | xylene       | 3 mins | xylene       |
| 3 mins   | xylene       | 2 mins   | xylene       | 2 mins | xylene       | 3 mins | xylene       |
| 3 mins   | 100% ethanol | 2 mins   | 100% ethanol | 2 mins | 100% ethanol | 3 mins | 100% ethanol |
| 3 mins   | 90% ethanol  | 2 mins   | 100% ethanol | 2 mins | 100% ethanol | 3 mins | 90% ethanol  |
| 3 mins   | 70% ethanol  | 2 mins   | 95% ethanol  | 2 mins | 95% ethanol  | 3 mins | 70% ethanol  |
| rinse    | water        | 2 mins   | water        | 2 mins | water        | rinse  | water        |
|          |              |          |              |        |              |        |              |
| 5 mins   | hematoxylin  | 5 mins   | hematoxylin  | 3 min  | hematoxylin  | 3 min  | hematoxylin  |
| rinse    | DI water     | rinse    | DI water     | 1 min  | water        | 1 min  | water        |
| rinse    | DI water     | rinse    | DI water     | 1 min  | acetic acid  | 1 min  | acetic acid  |
| 10-15 s  | Blueing      | 10-15 s  | Blueing      | 1 min  | water        | 1 min  | water        |
| rinse    | DI water     | rinse    | DI water     | 1 min  | Blueing      | 1 min  | Blueing      |
| rinse    | DI water     | rinse    | DI water     | 1 min  | water        | 1 min  | water        |
| rinse    | 100% ethanol | rinse    | 100% ethanol | 1 min  | 95% ethanol  | 1 min  | 95% ethanol  |
| 2-3 mins | Eosin Y      | 2-3 mins | Eosin Y      | 45 sec | eosin Y      | 45 sec | eosin Y      |
| rinse    | 100% ethanol | rinse    | 100% ethanol | 1 min  | 95% ethanol  | 1 min  | 95% ethanol  |
| rinse    | 100% ethanol | rinse    | 100% ethanol | 1 min  | 100% ethanol | 1 min  | 100% ethanol |
| rinse    | 100% ethanol | rinse    | 100% ethanol | 1 min  | 100% ethanol | 1 min  | 100% ethanol |
| rinse    | 100% ethanol | rinse    | 100% ethanol | 2 mins | xylene       | 2 mins | xylene       |
|          |              |          |              | 2 mins | xylene       | 2 mins | xylene       |

Procedures C and D are regressive stain procedures adapted from Leica Biosystems.<sup>27</sup> After completion of staining, slides were allowed to dry for 5 minutes, then mounted with DPX

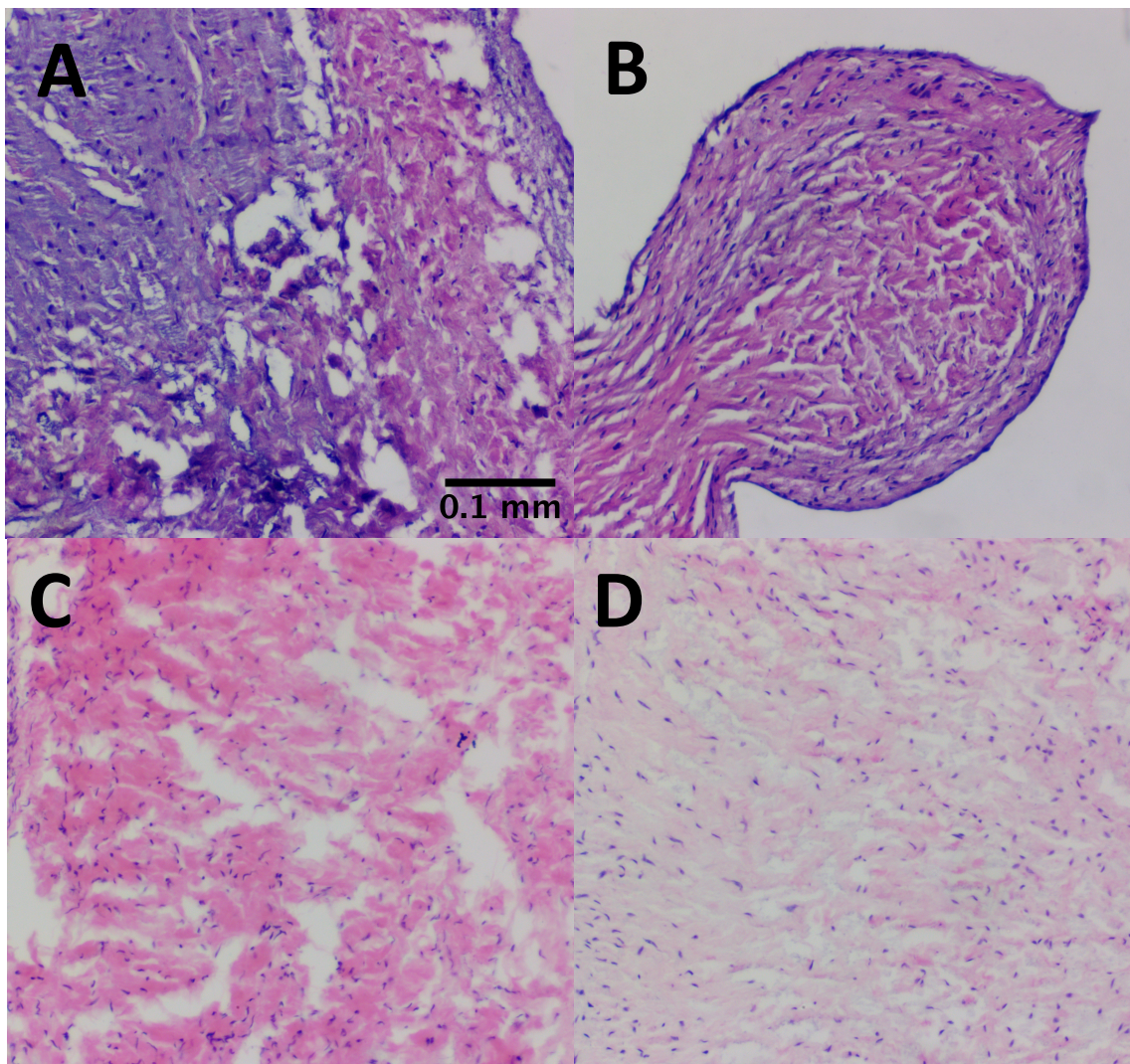
mountant and coverslips were applied. Slides were imaged using a microscope under 10x magnification.

## 3.2 Results

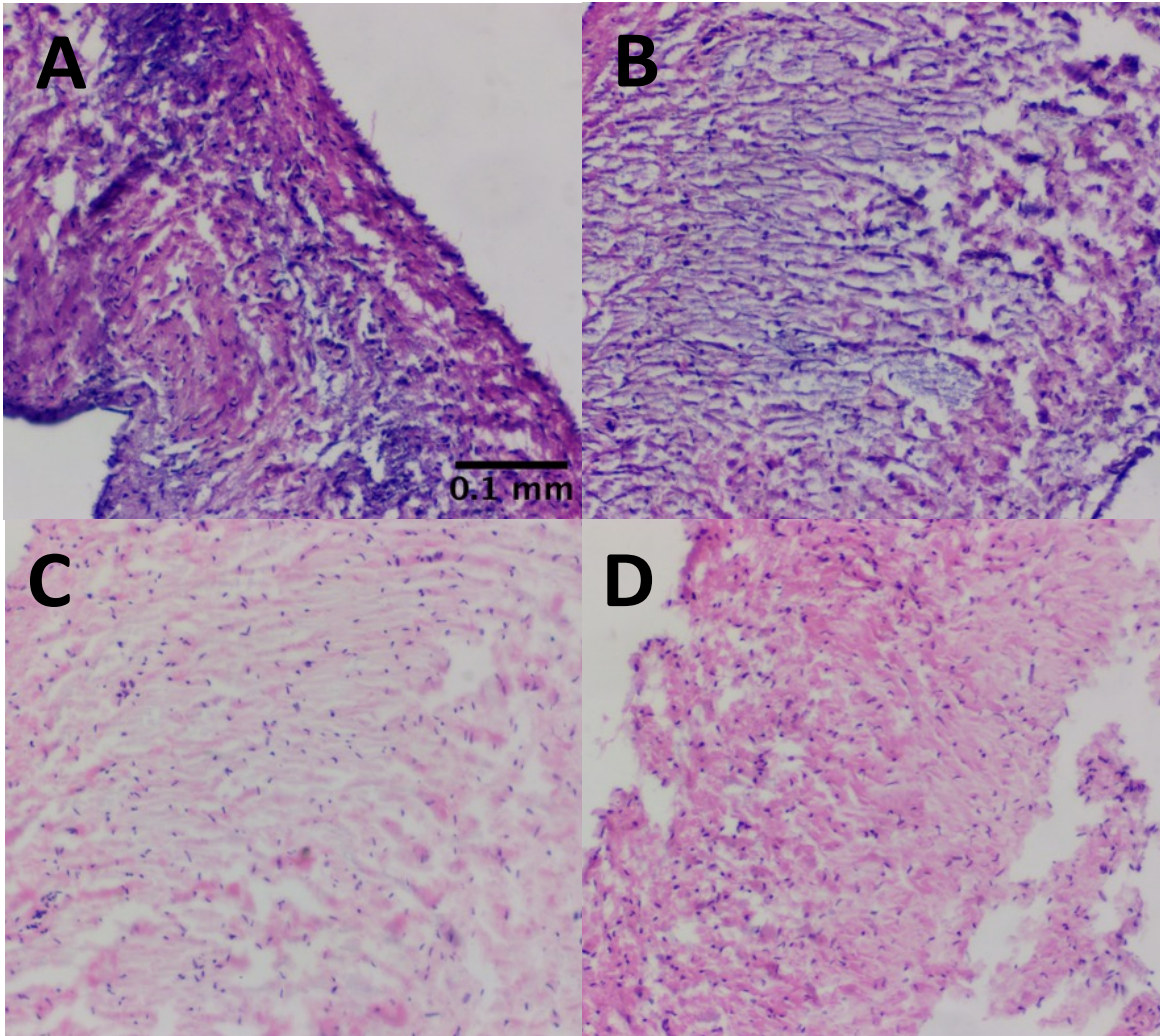
10x magnified images of progressively stained A and B for all three tricuspid leaflets showed dark background staining and poor contrast between nuclei and collagen, whereas regressively stained C and D showed light pink collagen staining with good contrast. There were no obvious differences between groups A and B or between groups C and D, suggesting that both the shorter and the longer deparaffinization procedures are effective.



**Figure 3-1.** 10X magnification of TVPL stained with H&E. Samples A and B were stained with a progressive procedure. Samples C and D were stained with a regressive procedure. Collagen is stained pink, nuclei are stained purple.



**Figure 3-2.** 10X magnification of TVAL stained with H&E. Samples A and B were stained with a progressive procedure. Samples C and D were stained with a regressive procedure. Collagen is stained pink, nuclei are stained purple.



**Figure 3-3.** 10X magnification of TVSL stained with H&E. Samples A and B were stained with a progressive procedure. Samples C and D were stained with a regressive procedure. Collagen is stained pink, nuclei are stained purple.

### 3.3 Discussion

Variation between labs and between lab workers, as well as many other factors such as stain oxygenation, solution contamination or dilution, solution pH, and tissue fixation quality frequently cause inconsistent histology results (Feldman). Results from this procedure may vary between individuals and between tissue samples. However, the results of this study consistently showed that regressively stained Tricuspid Valve leaflets show no hematoxylin background staining, as well as good contrast between nuclei and collagen. Additionally, there were no noticeable differences between longer and shorter deparaffinization times.

Treatment C (regressive stain, short deparaffinization time) was chosen as the optimal H&E staining procedure for this lab, and this procedure was used to determine the effectiveness of the decellularization study described in Chapter 4.

## Chapter 4 - Decellularization

In order to test the biaxial mechanical characteristics and collagen alignment of decellularized Tricuspid Valve Posterior Leaflets, a decellularization procedure was optimized to find the minimum treatment time necessary to remove cellular and genetic material with minimal damage to the Extracellular Matrix (ECM). Previous studies have reported that detergents Triton X-100 and sodium deoxycholate effectively decellularize heart valve tissue with minimal ECM damage, however no study has compared different exposure times to find minimum exposure time necessary to decellularize the tissue.<sup>28, 29, 30, 31, 32</sup>

### 4.1 Methods

Three porcine hearts were acquired from a local slaughterhouse and were dissected to excise the tricuspid valve leaflets, for a total of three tricuspid valve anterior leaflets (TVALs), three tricuspid valve posterior leaflets (TVPLs), and three tricuspid valve septal leaflets (TVSLs). Tissues were stored at 4 °C until the time of the experiment, then were thawed with 50 mM MgCl<sub>2</sub> PBS. Leaflets were sectioned into 9 circumferentially oriented strips, with the first strip closest to the annulus (Figure 4-1).



**Figure 4-1.** TVSL sectioned into 9 circumferentially oriented strips.

A detergent solution of 0.05% Triton X and 1% w/v sodium deoxycholate was made by adding 0.5 mL Triton X and 0.01 g sodium deoxycholate to 999.5 mL deionized water. An enzymatic solution of 100 ug/mL RNase and 0.2 mg/mL DNase was synthesized by adding 5 mg RNase and 10 mg DNase to 50 mL PBS with 50 mMol MgCl<sub>2</sub>.

Nine testing conditions were identified to determine the optimal combination of detergent and enzyme exposure. Tissues were exposed to combinations of 0, 12, or 24 hours of detergent and 0, 12, or 24 hours of enzymes. The exposure times for each tissue is presented in Table 4-1.

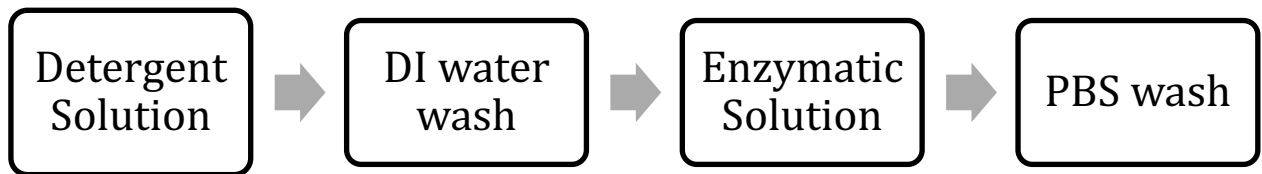
**Table 4-1.** Detergent exposure time (hours) and Enzyme exposure time (hours) for each tissue sample.

| Tissue | Detergent Exposure Time (h) | Enzyme Exposure Time (h) |
|--------|-----------------------------|--------------------------|
| 1      | 0                           | 0                        |
| 2      | 0                           | 12                       |
| 3      | 0                           | 24                       |
| 4      | 12                          | 0                        |
| 5      | 12                          | 12                       |
| 6      | 12                          | 24                       |
| 7      | 24                          | 0                        |
| 8      | 24                          | 12                       |
| 9      | 24                          | 24                       |

Immediately after the leaflets were sectioned, each tissue strip was placed in a microvial with detergent at room temperature for the designated time. After exposure to detergent, tissues were washed in DI water for 24 hours at room temperature to remove residual detergent. After



the DI water wash, each tissue was moved into a microvial with the enzyme solution for the designated time and maintained at 37 °C. Enzyme exposure was followed by a 24-hour wash in PBS at 37 °C. The steps of this procedure are shown in Figure 4-2. Immediately after the PBS bath, tissues were fixed with 10% neutral buffered formalin for 24 hours, and then stored in a 70% ethanol solution. This procedure was repeated for the TVAL, TVSL, and TVPL with  $n=3$  for each leaflet.

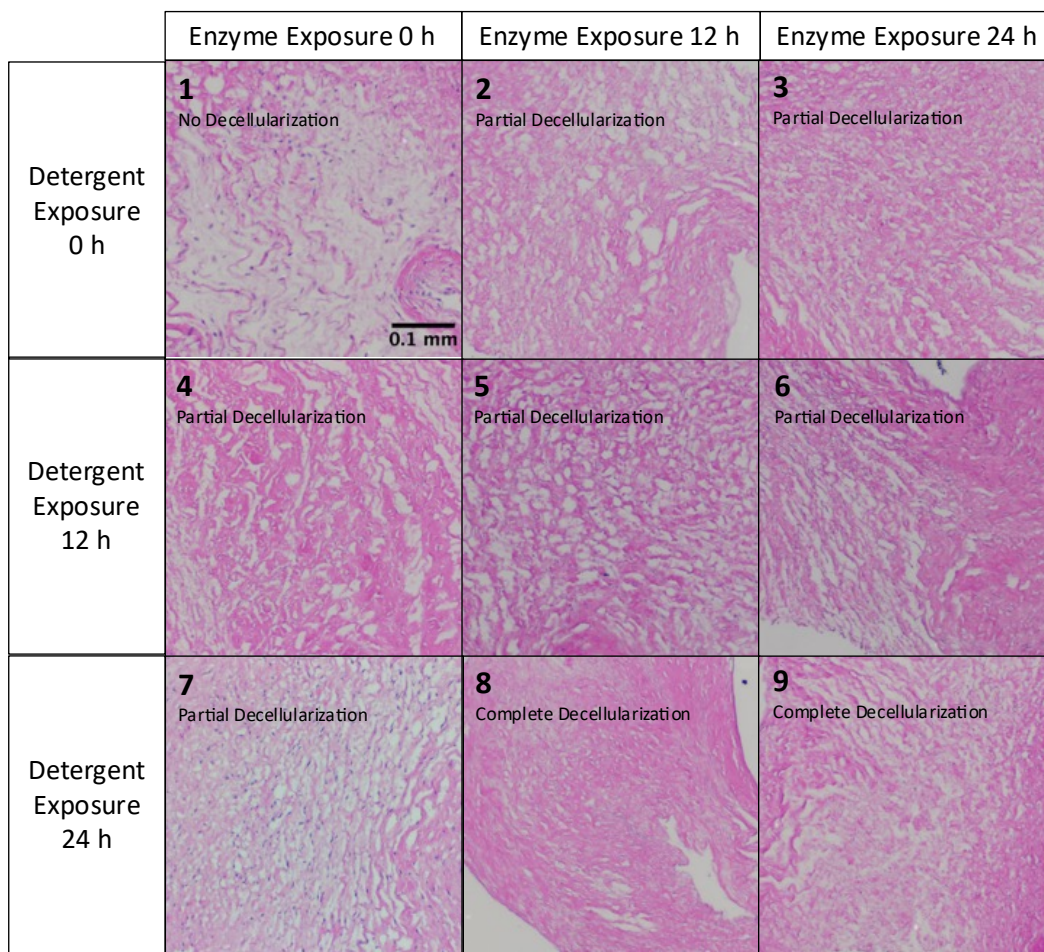


**Figure 4-2.** Steps of the decellularization procedure.

Tissues were stained with Hematoxylin and Eosin procedure detailed in section 3, and images were taken under 10x magnification. In addition to H&E staining, Alcian Blue staining was used to qualitatively examine the effects of the decellularization procedure on the GAG content in the leaflet. Sirius Red and Trichrome staining were used to examine the collagen content in response to the decellularization procedure, and pentachrome was used to view other components such as elastin, which stains purple.

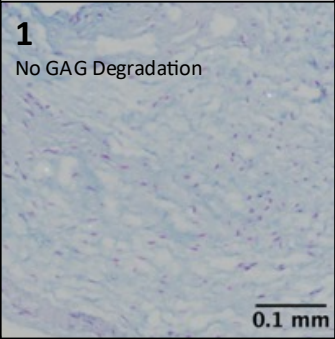
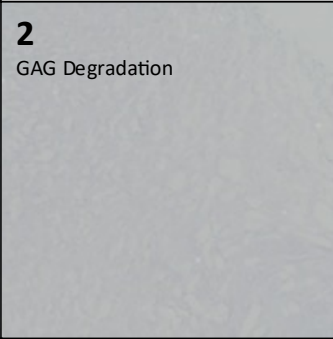
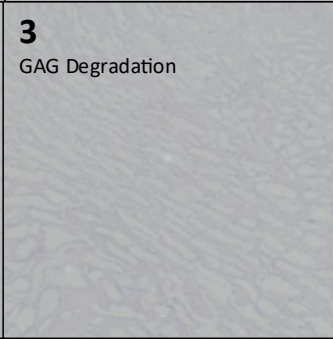
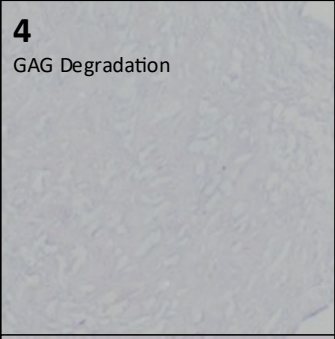

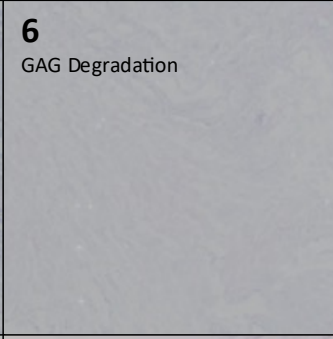
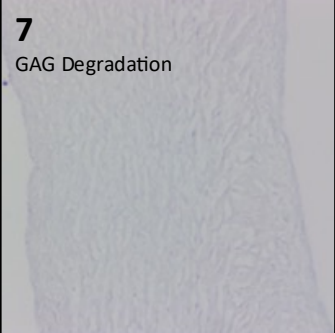
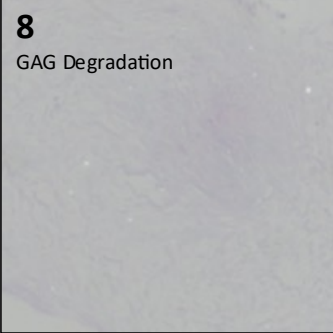
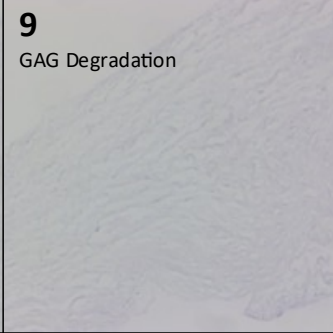
## 4.2 Results- TVSL

Images taken from H&E-stained tissues showed no decellularization in Tissue 1 (0 h detergents, 0 h enzymes). Tissues 2–7 showed partial decellularization, with a lower frequency of cells left in the ECM than in un-decellularized tissues. Tissues 8 and 9 showed complete decellularization with no visible cells in the extracellular matrix.



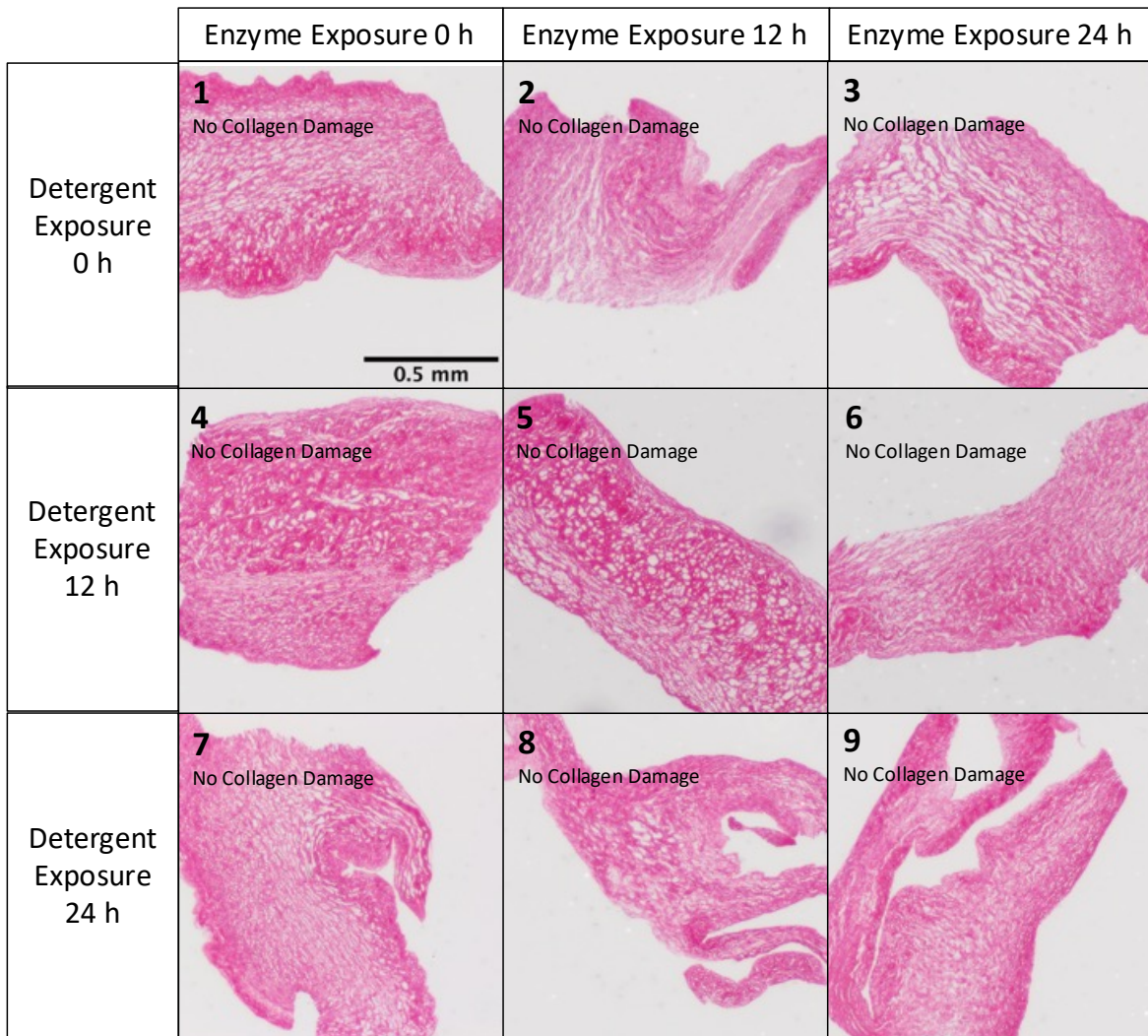
**Figure 4-3.** 10X magnification of H&E-stained tissues. Collagen is stained pink, and nuclei are stained purple.

Alcian Blue stained tissues showed no GAG degradation in the control tissue (tissue 1), but visible GAG degradation in every other group tested.

|                         | Enzyme Exposure 0 h  | Enzyme Exposure 12 h   | Enzyme Exposure 24 h  |
|-------------------------|--|--|---|
| Detergent Exposure 0 h  | <p><b>1</b><br/>No GAG Degradation</p>  <p>0.1 mm</p> | <p><b>2</b><br/>GAG Degradation</p>    | <p><b>3</b><br/>GAG Degradation</p>    |
| Detergent Exposure 12 h | <p><b>4</b><br/>GAG Degradation</p>                  | <p><b>5</b><br/>GAG Degradation</p>   | <p><b>6</b><br/>GAG Degradation</p>   |
| Detergent Exposure 24 h | <p><b>7</b><br/>GAG Degradation</p>                 | <p><b>8</b><br/>GAG Degradation</p>  | <p><b>9</b><br/>GAG Degradation</p>  |

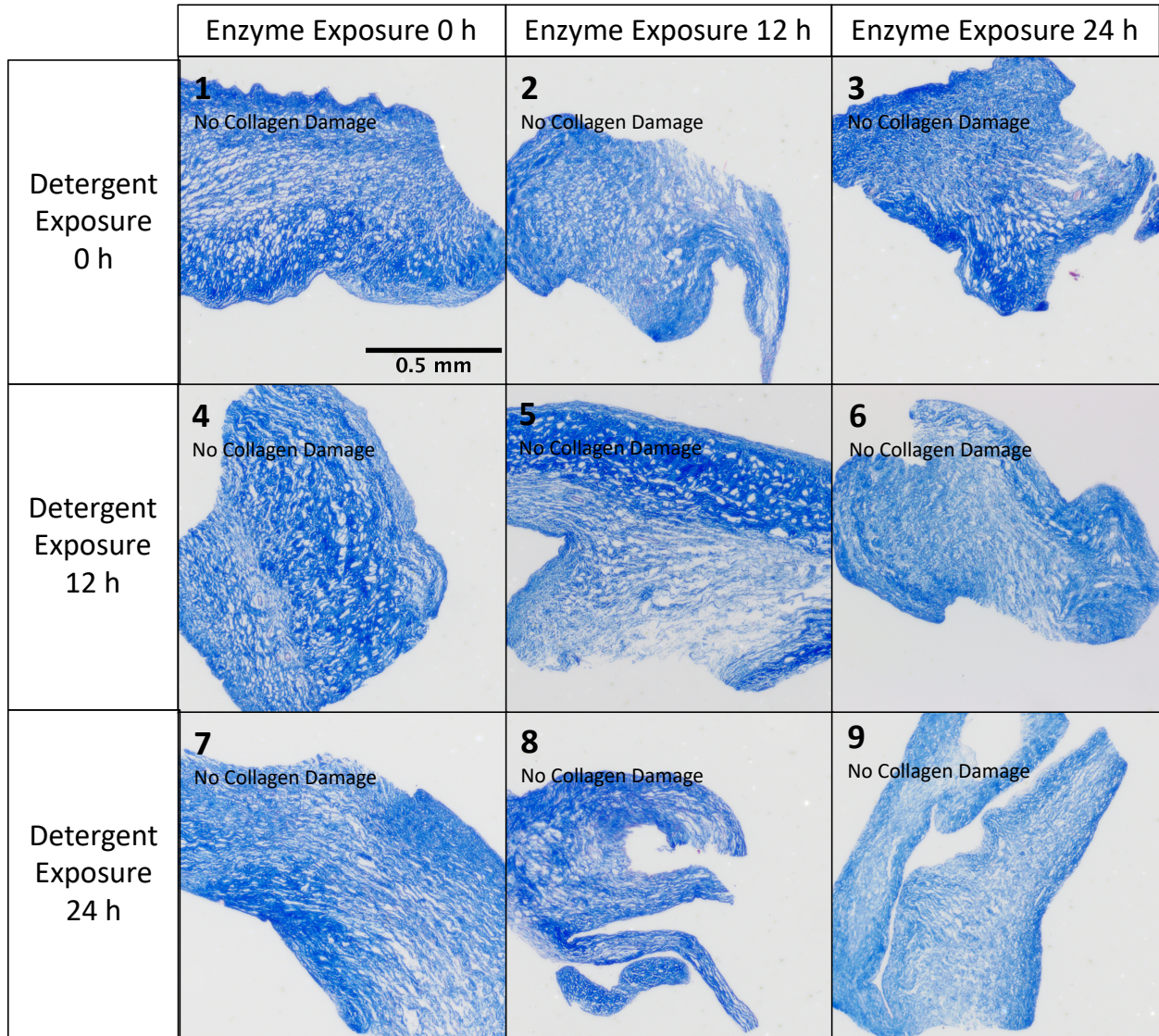
**Figure 4-4.** 10X magnification of Alcian Blue-stained tissues. GAGs are stained blue, and nuclei are stained purple.

Sirius Red stained tissues were imaged at magnification of 4X to visualize the collagen network of a greater area of the leaflet. No collagen damage was visible in the control group or any of the eight treatment groups.

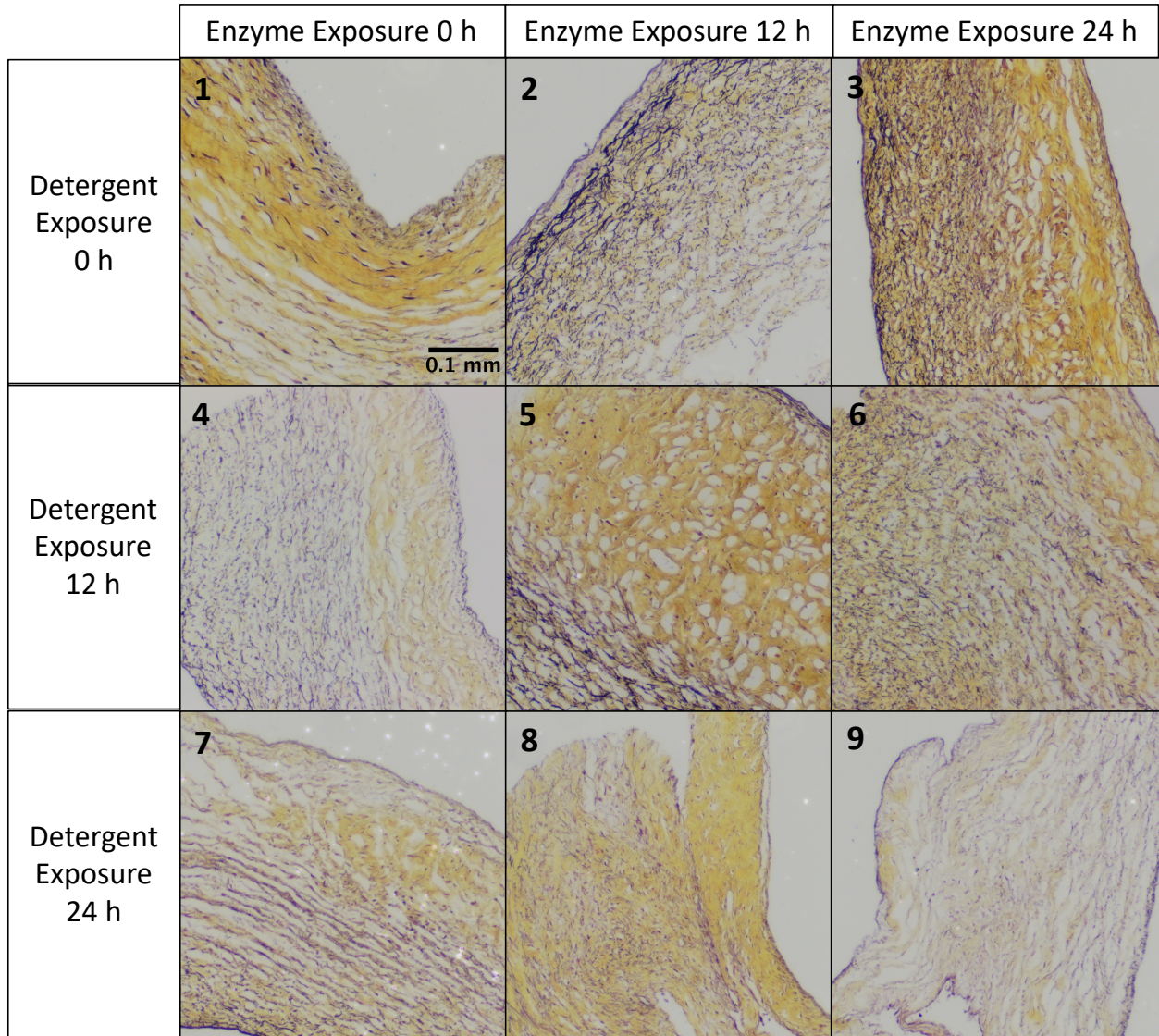


**Figure 4-5.** 4X magnification of Sirius Red-stained tissues. Collagen is stained dark pink.

Trichrome Stained tissues were imaged at 4X magnification, and no collagen damage was visible in the control group or treatment groups.



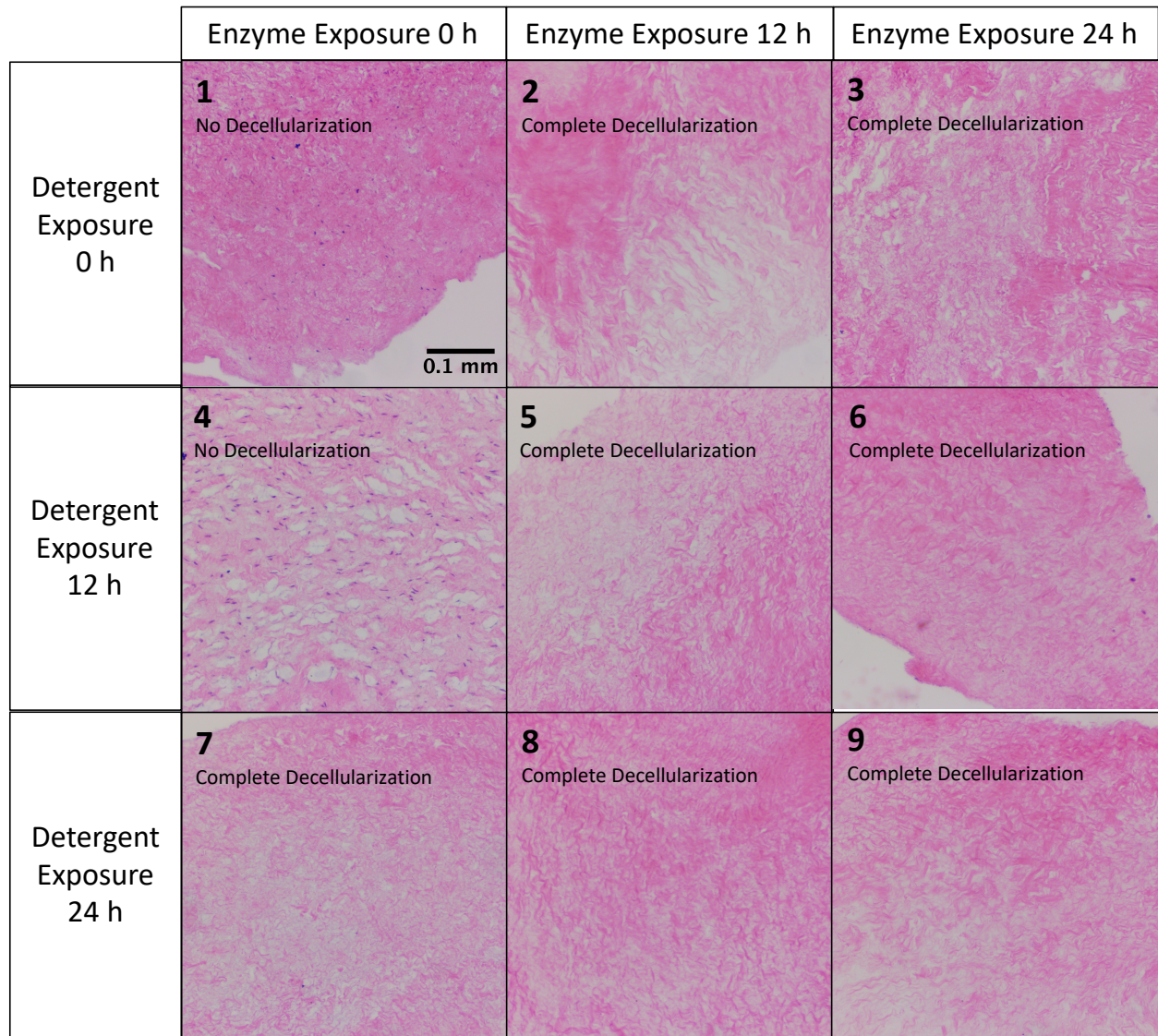
**Figure 4-6.** 4X magnification of Trichrome-stained tissues. Collagen is stained blue.



**Figure 4-7.** 10x magnification of Pentachrome-stained tissues. Nuclei and elastin are stained black. Collagen is stained yellow.

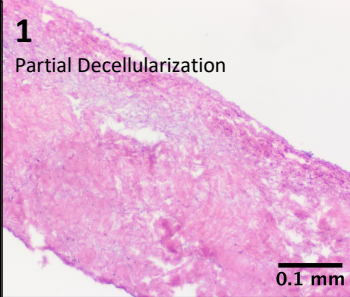








### 4.3 Results- TVAL

Decellularized TVAL leaflets underwent in-house H&E staining. TVAL tissues appear to decellularize more readily than TVSL tissues.



**Figure 4-8.** 10X magnification of H&E-stained tissues. Collagen is stained pink, and nuclei are stained purple.

### 4.4 Results- TVPL

|                         | Enzyme Exposure 0 h  | Enzyme Exposure 12 h  | Enzyme Exposure 24 h   |
|-------------------------|--|---|--|
| Detergent Exposure 0 h  | <b>1</b><br>Partial Decellularization<br>   | <b>2</b><br>Complete Decellularization<br>  | <b>3</b><br>Complete Decellularization<br>  |
| Detergent Exposure 12 h | <b>4</b><br>Partial Decellularization<br>   | <b>5</b><br>Complete Decellularization<br>  | <b>6</b><br>Complete Decellularization<br>  |
| Detergent Exposure 24 h | <b>7</b><br>Complete Decellularization<br> | <b>8</b><br>Complete Decellularization<br> | <b>9</b><br>Complete Decellularization<br> |

**Figure 4-9.** 10X magnification of H&E-stained tissues. Collagen is stained pink, and nuclei are stained purple.



## 4.5 Discussion

Histological results from the decellularization study consistently showed complete decellularization with no visible cell nuclei for both the TVAL and TVSL leaflets after decellularization protocol 8 (24-hour detergent exposure, 12-hour enzyme exposure) and protocol 9 (24 hour detergent exposure, 24 hour enzyme exposure). Protocol 8 was selected as the optimal decellularization treatment because a shorter treatment time is more ideal to prevent unnecessary ECM damage.

Trichrome and Sirius Red stained TVSLs showed no visible collagen damage. However, all TVSL decellularization groups showed visible GAG reduction compared to the control. Therefore, this treatment does not perfectly preserve the ECM of the leaflet.

## Chapter 5 - Analysis of Mechanical Characteristics and Collagen Alignment of Decellularized Tissues

In 2020, Meador et al. characterized the behavior of all three tricuspid valve leaflets under biaxial mechanical tension. Fibrous soft tissues exhibit a J-shaped stretch response which can be characterized by an initial linear stretch at low membrane tension, a non-linear transition period in which collagen fibers uncrimp and engage, and an almost vertical linear segment with little tissue stretch. Meador's study showed consistent results for all three leaflets in the circumferential direction, but not in the radial direction, suggesting some mechanical anisotropy between the leaflets.<sup>33</sup>

Tricuspid leaflet collagen fiber network response to physiological and pathological loading scenarios has been investigated in-depth, but the effects of decellularization on these properties has never been reported. Changes in the collagen fiber architecture due to decellularization methods could provide evidence as to how the engineered leaflets will behave *in vivo*. Polarized spatial frequency domain imaging (pSFDI) provides insight into the alignment of collagen fibers in the leaflet through two values of interest: the  $\theta_{\text{Fiber}}$ , which is the mean angle of a group of fibers, and the degree of optical anisotropy (DOA), or the dispersion of local collagen fibers (Figure 5-1).

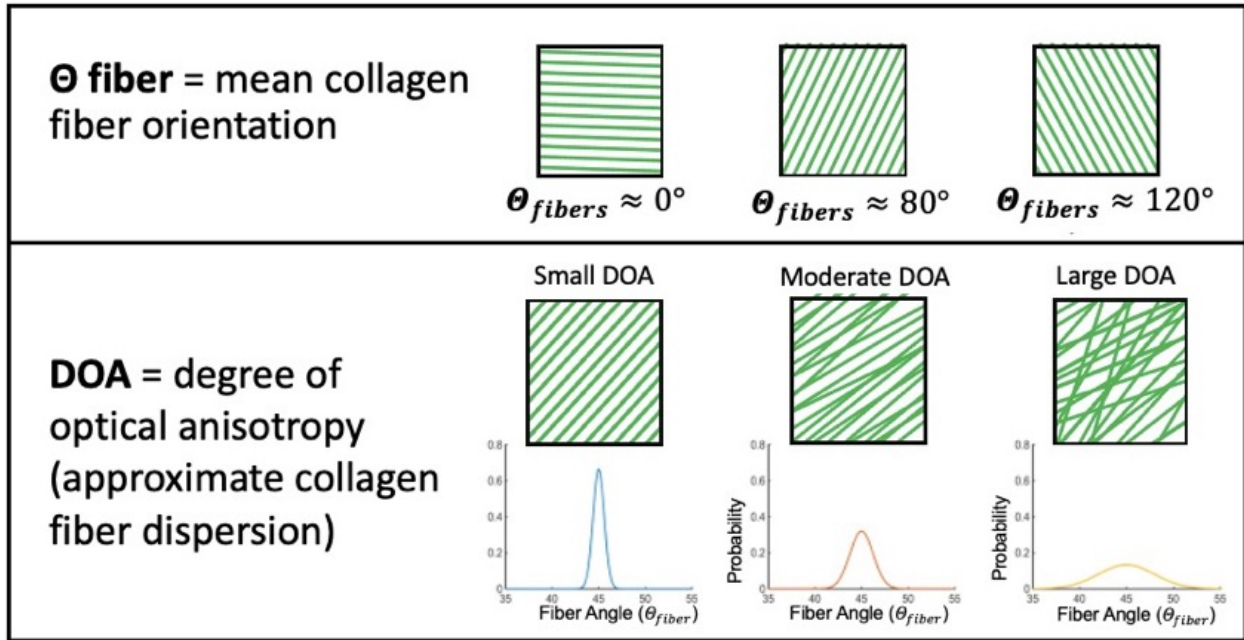
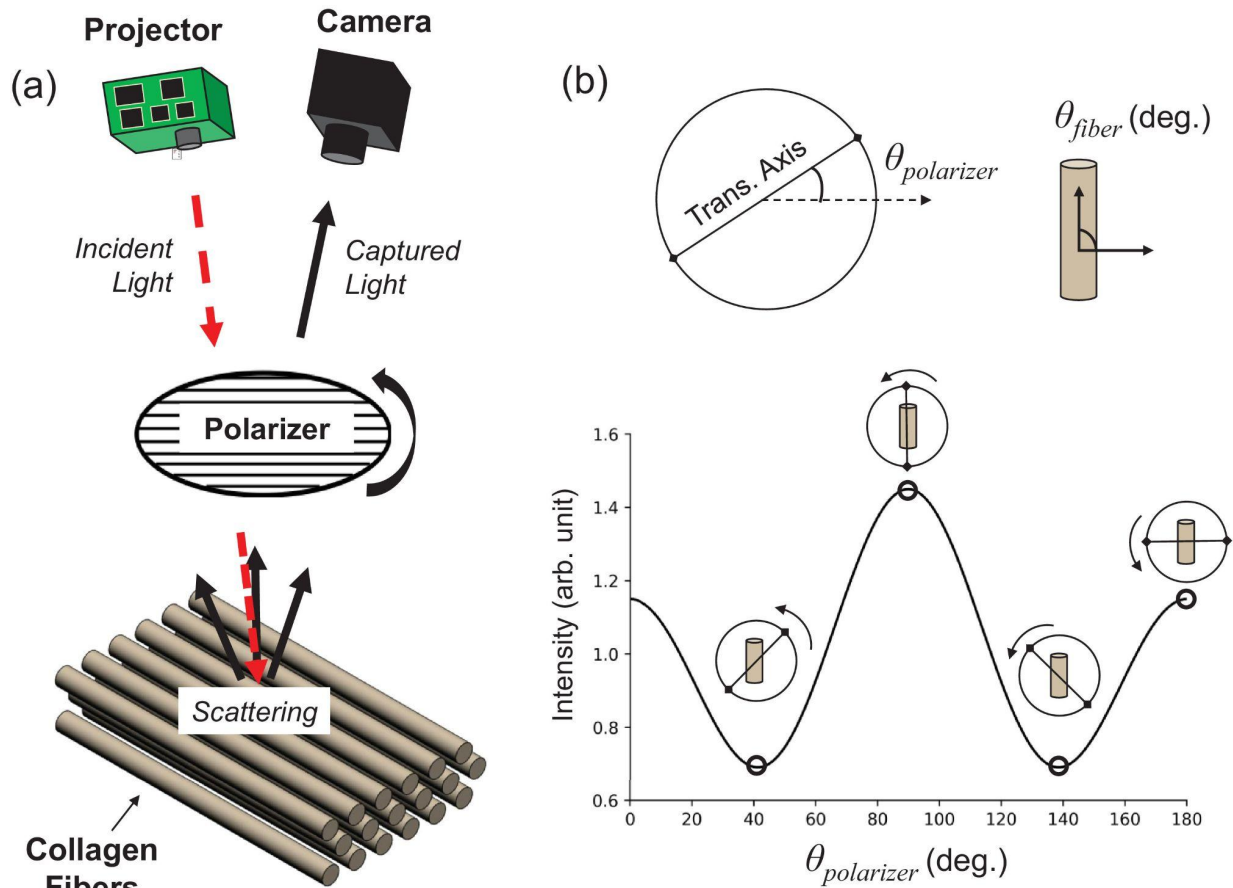


Figure 5-1. Representation of  $\theta_{Fiber}$  and DOA parameters.

pSFDI analysis of collagen architecture employs birefringent collagen scattering, in which light is passed through a polarizer at an angle  $\theta_{\text{Polarizer}}$ , reflected from the tissue back through the same polarizer, and the intensity of the reflected light is measured<sup>34</sup> (Figure 5-2).



**Figure 5-2.** a) Schematic of system setup. b) Depiction of  $\theta_{\text{Polarizer}}$  and  $\theta_{\text{Fiber}}$ , as well as bimodal intensity peak. (Image from Jett et al. 2021<sup>34</sup>)

The polarizer lens is rotated  $180^\circ$  and the intensity is measured every  $5^\circ$ , and results are represented in a graph showing measured light intensity vs.  $\theta_{\text{Polarizer}}$ . The peak measured intensity occurs when  $\theta_{\text{Fiber}} = \theta_{\text{Polarizer}}$ , meaning that the polarized light is parallel with the collagen fibers. The smaller peak occurs when  $\theta_{\text{Fiber}} = \theta_{\text{Polarizer}} + 90^\circ$ , meaning polarized light is perpendicular to collagen fibers.

## 5.1 Methods

In this study, the biaxial mechanical characteristics and collagen alignment of TVPLs were analyzed before and after the decellularization procedure that was optimized in chapter 4. Leaflets were mounted to the biaxial tester with four rakes to form a testing square of 7.5 mm and submerged in PBS for the duration of the procedure. The circumferential direction of the leaflet was aligned with the  $X$  direction, while the radial leaflet aligned with the  $Y$  direction. Leaflets underwent 10 preconditioning stretch cycles to return them to their *in vivo* configuration, then were subjected to seven different loading conditions with different ratios of circumferential to radial forces (1:1, 1:0.75, 1:0.5, 1:0.25, 0.75:1, 0.5:1, 0.25:1). Tissue stretch in response to these stresses was collected. With the tissue still mounted to the biaxial tester, pSFDI was used to evaluate the collagen alignment under different circumferential to radial force ratios (unloaded, 1:1, 1:0.25, 0.25:1).

Immediately after biaxial and pSFDI characterization, experimental group tissues underwent the optimized decellularization procedure of four parts:

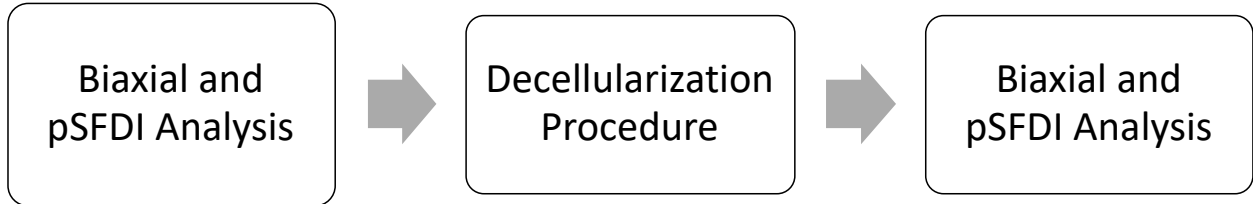
1. 24 hours in 0.05% Triton X and 1% w/v sodium deoxycholate
2. 24-hour DI water wash
3. 12-hour exposure to 100 ug/mL RNase and 0.2 mg/mL DNase
4. 24-hour PBS wash

Control group tissues underwent an extensive washing procedure to eliminate the possibility that observed results could be due to prolonged periods in solution:

1. 24 hours in DI water
2. 24 hours in DI water
3. 12 hours in PBS

4. 24 hours in PBS

Immediately following the final washing step for both experimental and control groups, tissues were remounted to the biaxial tester with a testing size of 6.5x6.5 mm to avoid the presence of fine holes in the testing region. The tissues underwent preconditioning, biaxial testing, and pSFDI characterization according to the same procedure described above (Figure 5-3).



**Figure 5-3.** Summary of the biaxial/pSFDI, decellularization, biaxial/pSFDI pipeline.

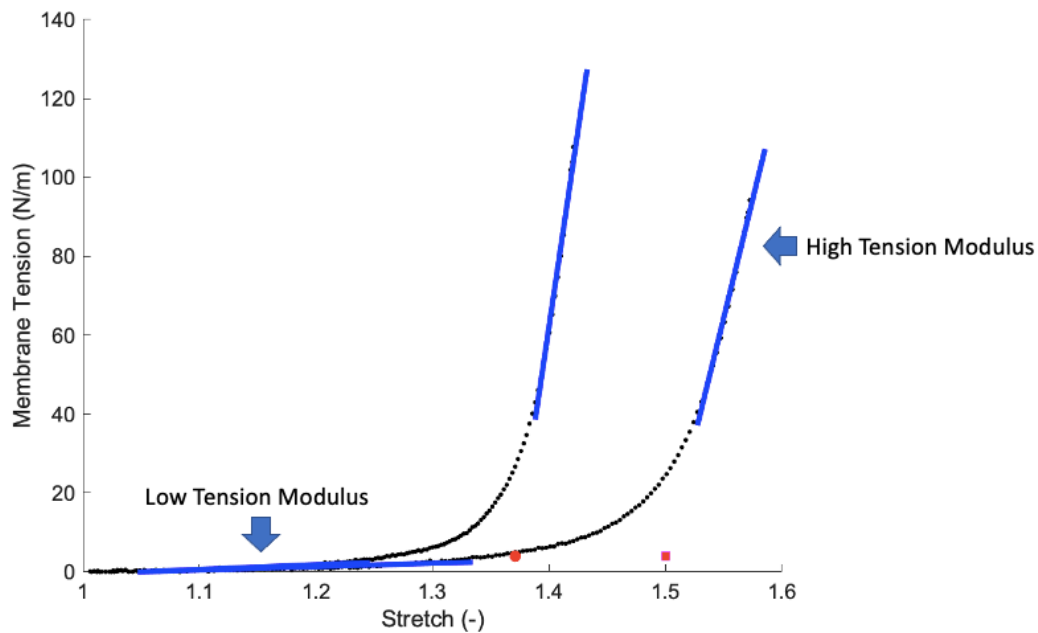
A summary of the Biaxial/pSFDI analysis of decellularized tissues and control group tissues is shown in Table 5-1. This procedure was repeated with  $n=5$  for each group.

**Table 5-1.** Summary of the decellularized group procedure vs. the control group procedure.

| Decellularized Group |                       | Control Group |                       |
|----------------------|-----------------------|---------------|-----------------------|
| ~3 h                 | Biaxial/pSFDI testing | ~3 h          | Biaxial/pSFDI testing |
| 24 h                 | Solution 1            | 24 h          | DI water wash         |
| 24 h                 | DI water wash         | 24 h          | DI water wash         |
| 12 h                 | Solution 2            | 12 h          | PBS                   |
| 24 h                 | PBS wash              | 24 h          | PBS wash              |
| ~3 h                 | Biaxial/pSFDI testing | ~3 h          | Biaxial/pSFDI testing |

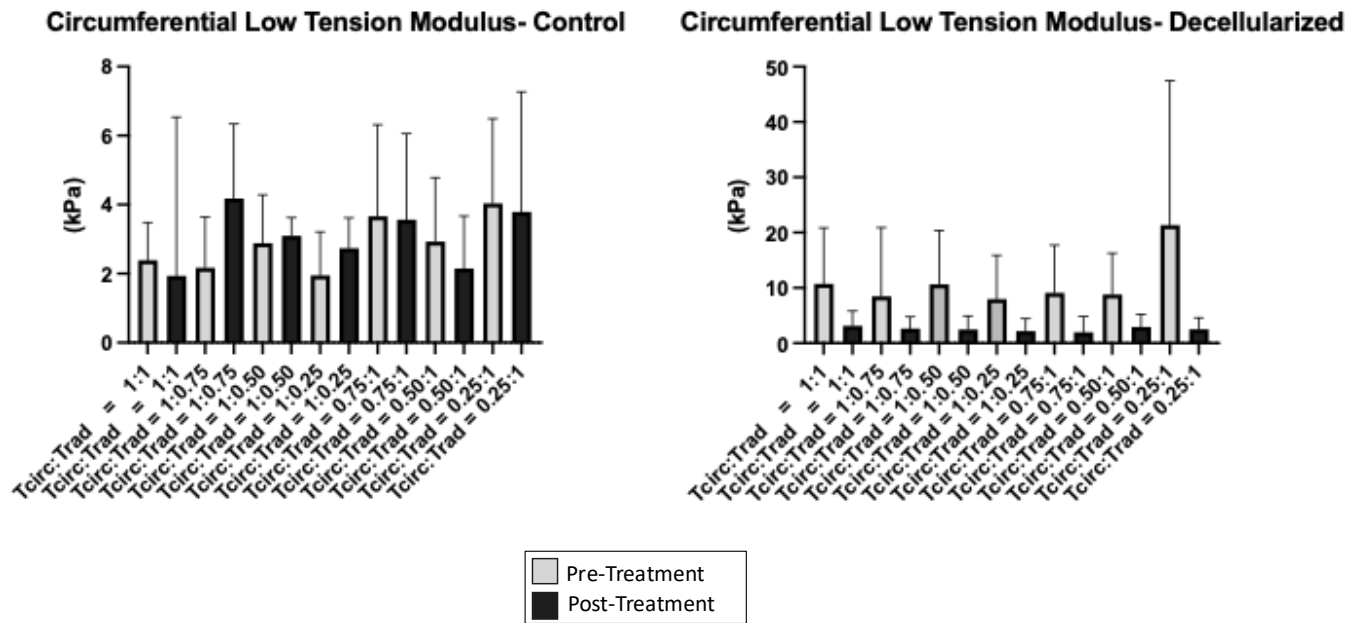
## 5.2 Results- Biaxial Testing

Several parameters were evaluated to discover whether the decellularization treatment has a statistically significant impact on the biaxial mechanics and collagen alignment of the TVPL. These parameters include high tension and low-tension moduli in both the circumferential and radial directions, peak stretch in both the circumferential and radial directions, average  $\theta_{\text{Fiber}}$  across the tissue, and average DOA across the tissue. The high-tension modulus of the tissue is the approximated slope of the high tension, linear portion of the tension-stretch curve that is correlated with full collagen engagement and stretching. The low-tension modulus is the approximated slope of the low-tension linear region, correlated with collagen fiber uncrimping (Figure 5-4).



**Figure 5-4.** Membrane tension-stretch curve with high-tension moduli and low-tension moduli fitted to both the circumferential curve and the radial curve.

For each of the seven loading ratios ( $T_{\text{circ}}:T_{\text{rad}} = 1:1, 1:0.75, 1:0.5, 1:0.25, 0.75:1, 0.5:1, 0.25:1$ ), the pre-treatment value and the post-treatment value for the low-tension modulus in the circumferential direction were compared to the using a paired  $t$  test. No statistically significant results were found from pre-treatment to post-treatment for any of the loading ratios, for either the control group or the decellularized group (Figure 5-5).

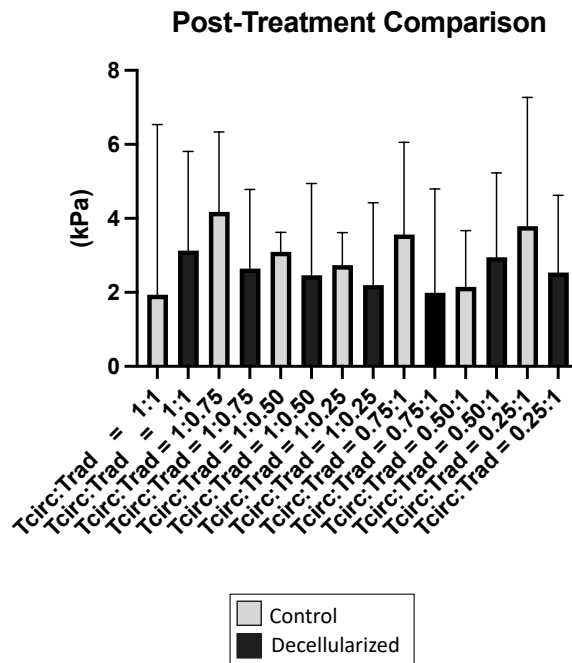


**Figure 5-5.** Circumferential low-tension modulus for control and decellularized treatment groups. Pre-treatment values are compared to post-treatment values with a paired  $t$  test.

Statistical significance is indicated with \* =  $p < 0.05$  , and \*\* =  $p < 0.005$ .



Additionally, for the low-tension modulus in the circumferential direction, the post-treatment value for the control group was compared to the post-treatment value for the decellularized group for each loading protocol ( $T_{\text{circ}}:T_{\text{rad}} = 1:1, 1:0.75, 1:0.5, 1:0.25, 0.75:1, 0.5:1, 0.25:1$ ) using a paired  $t$  test. There were no statistically significant results from control group to decellularized group for any of the loading ratios (Figure 5-6).



**Figure 5-6.** Circumferential low-tension modulus post-treatment values from the control group are compared to the post-treatment values from the decellularized group with a paired  $t$  test.

Statistical significance is indicated with \* =  $p < 0.05$  , and \*\* =  $p < 0.005$ .

The circumferential low-tension modulus values were averaged and the percent change calculated between the pre-treatment and post-treatment values (Tables 5-2 and 5-3).

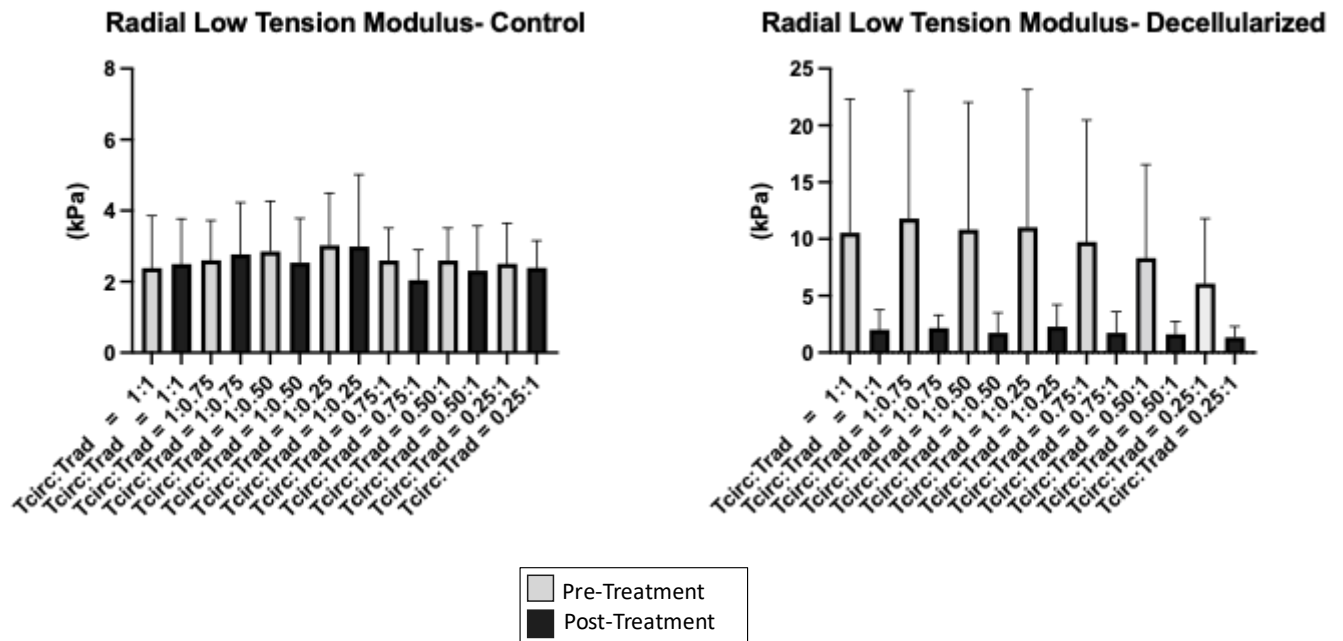
**Table 5-2.** Circumferential low-tension modulus values and % change from pre-treatment to post-treatment for the control group.

| <b>Control</b>                |                 |                 |                 |                 |                 |            |            |                 |
|-------------------------------|-----------------|-----------------|-----------------|-----------------|-----------------|------------|------------|-----------------|
|                               | <b>Tissue 1</b> | <b>Tissue 2</b> | <b>Tissue 3</b> | <b>Tissue 4</b> | <b>Tissue 5</b> | <b>AVG</b> | <b>SEM</b> | <b>% Change</b> |
| <b>1:1, Pre-Treatment</b>     | 4.10902         | 1.083965        | 2.055272        | 2.320227        | 2.383383        | 2.39037349 | 0.4887592  | -19%            |
| <b>1:1, Post-Treatment</b>    | 1.045986        | 2.295636        | -4.880797       | 3.344397        | 7.876598        | 1.93636383 | 2.05747984 |                 |
| <b>1:0.75, Pre-Treatment</b>  | 4.29306         | 0.795558        | 1.9528          | 2.92972         | 0.879645        | 2.17015655 | 0.65900841 | 92%             |
| <b>1:0.75, Post-Treatment</b> | 2.234037        | 1.906193        | 6.604673        | 4.017294        | 6.124316        | 4.17730266 | 0.96547432 |                 |
| <b>1:0.50, Pre-Treatment</b>  | 3.793949        | 1.277352        | 2.359854        | 2.192533        | 4.799337        | 2.884605   | 0.62572724 | 7%              |
| <b>1:0.50, Post-Treatment</b> | 2.423478        | 3.125149        | 2.868005        | 3.86635         | 3.199697        | 3.09653573 | 0.23551094 |                 |
| <b>1:0.25, Pre-Treatment</b>  | 3.814634        | 0.883937        | 1.011189        | 2.677745        | 1.364653        | 1.95043175 | 0.56422338 | 40%             |
| <b>1:0.25, Post-Treatment</b> | 2.327755        | 2.471036        | 1.722098        | 3.139477        | 4.026846        | 2.73744218 | 0.39331492 |                 |
| <b>0.75:1, Pre-Treatment</b>  | 5.236472        | 1.587886        | 1.240901        | 2.747819        | 7.492967        | 3.6612089  | 1.18647943 | -3%             |
| <b>0.75:1, Post-Treatment</b> | 2.273574        | 0.382021        | 6.875435        | 3.342338        | 4.95954         | 3.56658178 | 1.1124843  |                 |
| <b>0.50:1, Pre-Treatment</b>  | 3.243477        | 0.810718        | 1.773563        | 3.122644        | 5.712538        | 2.93258812 | 0.82784553 | -27%            |
| <b>0.50:1, Post-Treatment</b> | 2.3203          | 2.625157        | -0.495502       | 3.226182        | 3.076815        | 2.15059055 | 0.68083063 |                 |
| <b>0.25:1, Pre-Treatment</b>  | 6.171801        | 0.410717        | 4.813986        | 2.737635        | 6.048603        | 4.03654822 | 1.09649232 | -6%             |
| <b>0.25:1, Post-Treatment</b> | 1.303817        | 8.231226        | -0.475985       | 4.042148        | 5.861461        | 3.79253327 | 1.55657838 |                 |

**Table 5-3.** Circumferential low-tension modulus values and % change from pre-treatment to post-treatment for the decellularized group.

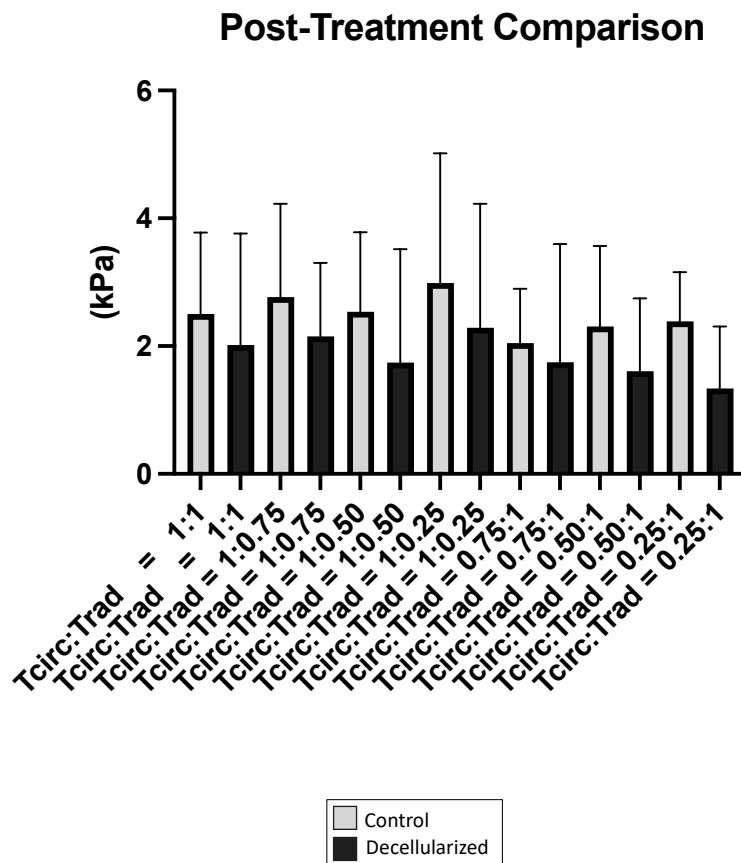
| <b>Decellularized</b>         |                 |                 |                 |                 |                 |            |            |                 |
|-------------------------------|-----------------|-----------------|-----------------|-----------------|-----------------|------------|------------|-----------------|
|                               | <b>Tissue 1</b> | <b>Tissue 2</b> | <b>Tissue 3</b> | <b>Tissue 4</b> | <b>Tissue 5</b> | <b>AVG</b> | <b>SEM</b> | <b>% Change</b> |
| <b>1:1, Pre-Treatment</b>     | 2.360227        | 21.93409        | 21.59979        | 4.657377        | 3.06517         | 10.7233314 | 4.52417538 | -71%            |
| <b>1:1, Post-Treatment</b>    | 7.901501        | 1.448877        | 2.101227        | 2.212084        | 1.979105        | 3.1285586  | 1.20039347 |                 |
| <b>1:0.75, Pre-Treatment</b>  | 2.791896        | 23.49269        | 18.85616        | 3.949049        | -6.783163       | 8.46132727 | 5.56278755 | -69%            |
| <b>1:0.75, Post-Treatment</b> | 5.570401        | 4.130886        | 1.982082        | 0.999115        | 0.544194        | 2.64533562 | 0.95727776 |                 |
| <b>1:0.50, Pre-Treatment</b>  | 2.964883        | 25.8032         | 15.10627        | 4.376057        | 4.99433         | 10.6489474 | 4.3582549  | -77%            |
| <b>1:0.50, Post-Treatment</b> | 6.8552          | 1.324792        | 1.464577        | 1.841201        | 0.830711        | 2.46329633 | 1.10983755 |                 |
| <b>1:0.25, Pre-Treatment</b>  | 2.456967        | 20.87125        | 10.26306        | 2.574509        | 3.826433        | 7.99844439 | 3.52399187 | -72%            |
| <b>1:0.25, Post-Treatment</b> | 6.073611        | 0.393309        | 1.282694        | 1.484858        | 1.765479        | 2.19999018 | 0.99525577 |                 |
| <b>0.75:1, Pre-Treatment</b>  | 3.143012        | 17.85563        | 19.19191        | 3.707836        | 1.650927        | 9.10986254 | 3.86365741 | -78%            |
| <b>0.75:1, Post-Treatment</b> | 6.04739         | 0.949821        | 1.644706        | 2.923546        | -1.599556       | 1.99318145 | 1.25339513 |                 |
| <b>0.50:1, Pre-Treatment</b>  | 3.433077        | 15.44756        | 18.24141        | 2.35451         | 4.612984        | 8.81790757 | 3.32571757 | -67%            |
| <b>0.50:1, Post-Treatment</b> | 6.584361        | 1.310973        | 2.453584        | 3.533277        | 0.864518        | 2.9493426  | 1.02056021 |                 |
| <b>0.25:1, Pre-Treatment</b>  | 3.10537         | 16.78784        | 67.24731        | 10.32748        | 9.38431         | 21.3704595 | 11.6724342 | -88%            |
| <b>0.25:1, Post-Treatment</b> | 5.49475         | 0.893289        | 2.393125        | 3.566916        | 0.341549        | 2.53792591 | 0.93143698 |                 |

For each of the seven loading ratios ( $T_{\text{circ}}:T_{\text{rad}} = 1:1, 1:0.75, 1:0.5, 1:0.25, 0.75:1, 0.5:1, 0.25:1$ ), the pre-treatment value and the post-treatment value for the low tension modulus in the radial direction were compared to the using a paired  $t$  test. No statistically significant results were found from pre-treatment to post-treatment for any of the loading ratios, for either the control group or the decellularized group.



**Figure 5-7.** Radial low-tension modulus for control and decellularized treatment groups. Pre-treatment values are compared to post-treatment values with a paired  $t$  test. Statistical significance is indicated with  $*$  =  $p < 0.05$  , and  $**$  =  $p < 0.005$ .

Additionally for the low-tension modulus in the radial direction, the post-treatment value for the control group was compared to the post-treatment value for the decellularized group for each loading protocol ( $T_{\text{circ}}:T_{\text{rad}} = 1:1, 1:0.75, 1:0.5, 1:0.25, 0.75:1, 0.5:1, 0.25:1$ ) using a paired  $t$  test. There were no statistically significant results from control group to decellularized group for any of the loading ratios (Figure 5-8).



**Figure 5-8.** Radial low-tension modulus post-treatment values from the control group are compared to the post-treatment values from the decellularized group with a paired  $t$  test.

Statistical significance is indicated with \* =  $p < 0.05$  , and \*\* =  $p < 0.005$ .

The radial low-tension modulus values were averaged and the percent change calculated between the pre-treatment and post-treatment values (Tables 5-4 and 5-5).

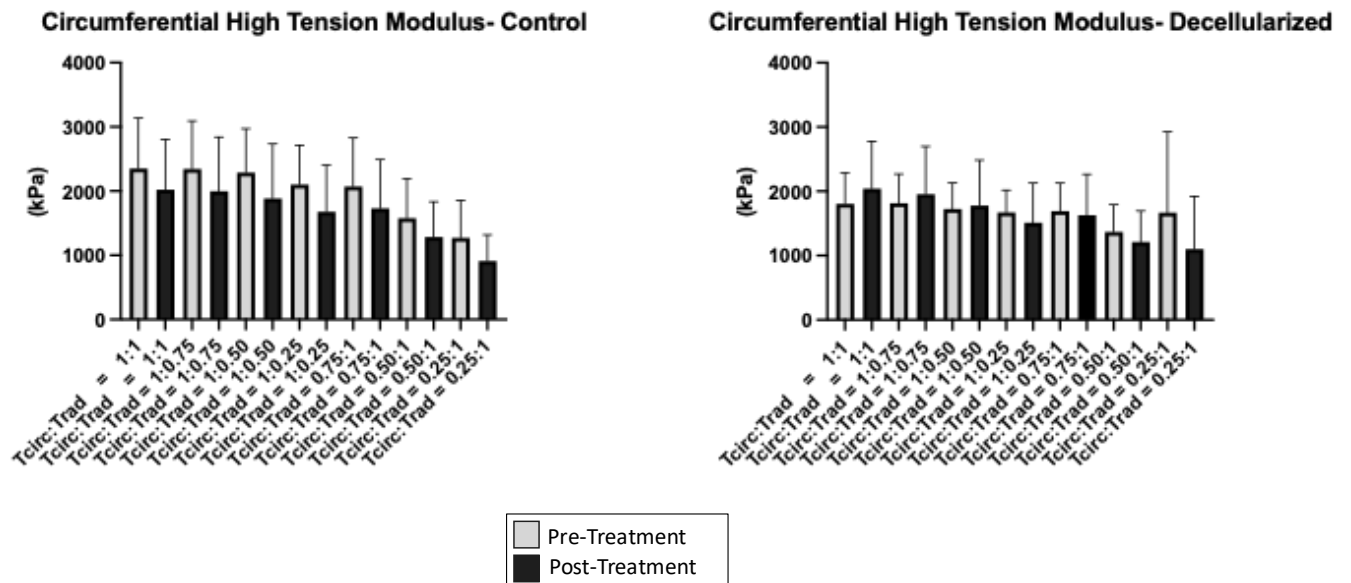
**Table 5-4.** Radial low-tension modulus values and % change from pre-treatment to post-treatment for the control group.

| <b>Control</b>                |                 |                 |                 |                 |                 |            |            |                 |
|-------------------------------|-----------------|-----------------|-----------------|-----------------|-----------------|------------|------------|-----------------|
|                               | <b>Tissue 1</b> | <b>Tissue 2</b> | <b>Tissue 3</b> | <b>Tissue 4</b> | <b>Tissue 5</b> | <b>AVG</b> | <b>SEM</b> | <b>% Change</b> |
| <b>1:1, Pre-Treatment</b>     | 3.50633         | 1.442641        | 0.70754         | 4.27581         | 1.970618        | 2.38058766 | 0.65977533 | 5%              |
| <b>1:1, Post-Treatment</b>    | 2.44651         | 1.323019        | 4.44708         | 2.864702        | 1.398009        | 2.49586387 | 0.57125175 |                 |
| <b>1:0.75, Pre-Treatment</b>  | 3.598895        | 1.434463        | 1.434904        | 3.730244        | 2.804684        | 2.60063765 | 0.50165032 | 6%              |
| <b>1:0.75, Post-Treatment</b> | 2.287847        | 1.561701        | 5.128825        | 3.15527         | 1.703689        | 2.76746651 | 0.65352645 |                 |
| <b>1:0.50, Pre-Treatment</b>  | 3.543925        | 2.199993        | 0.719156        | 4.410121        | 3.360227        | 2.84668438 | 0.63791816 | -11%            |
| <b>1:0.50, Post-Treatment</b> | 1.97266         | 2.293691        | 4.440287        | 2.883935        | 1.108571        | 2.53982866 | 0.55501874 |                 |
| <b>1:0.25, Pre-Treatment</b>  | 3.410426        | 2.032044        | 1.3429          | 5.187901        | 3.14353         | 3.02336019 | 0.6578811  | -1%             |
| <b>1:0.25, Post-Treatment</b> | 1.973418        | 1.100605        | 6.303608        | 3.411096        | 2.146681        | 2.9870818  | 0.9075162  |                 |
| <b>0.75:1, Pre-Treatment</b>  | 3.435117        | 1.862695        | 1.568189        | 3.61238         | 2.51856         | 2.5993882  | 0.40848598 | -21%            |
| <b>0.75:1, Post-Treatment</b> | 2.023383        | 0.885922        | 3.258331        | 2.219369        | 1.83879         | 2.04515871 | 0.38006764 |                 |
| <b>0.50:1, Pre-Treatment</b>  | 3.304025        | 1.584442        | 1.658696        | 2.993139        | 3.455614        | 2.59918315 | 0.40618307 | -11%            |
| <b>0.50:1, Post-Treatment</b> | 1.718046        | 1.372318        | 4.25896         | 2.885809        | 1.304997        | 2.30802613 | 0.56434341 |                 |
| <b>0.25:1, Pre-Treatment</b>  | 3.55108         | 1.312265        | 1.218272        | 3.464652        | 2.955339        | 2.5003216  | 0.51459681 | -4%             |
| <b>0.25:1, Post-Treatment</b> | 1.709833        | 2.387684        | 2.89914         | 3.378687        | 1.569117        | 2.38889225 | 0.34447053 |                 |

**Table 5-5.** Radial low-tension modulus values and % change from pre-treatment to post-treatment for the decellularized group.

| <b>Decellularization</b>      |                 |                 |                 |                 |                 |            |            |                 |
|-------------------------------|-----------------|-----------------|-----------------|-----------------|-----------------|------------|------------|-----------------|
|                               | <b>Tissue 1</b> | <b>Tissue 2</b> | <b>Tissue 3</b> | <b>Tissue 4</b> | <b>Tissue 5</b> | <b>AVG</b> | <b>SEM</b> | <b>% Change</b> |
| <b>1:1, Pre-Treatment</b>     | 1.410569        | 17.72023        | 27.89563        | 2.946576        | 2.788101        | 10.552221  | 4.29678673 | -81%            |
| <b>1:1, Post-Treatment</b>    | 4.243025        | 0.749647        | 3.420299        | 0.175165        | 1.503526        | 2.01833209 | 0.63735452 |                 |
| <b>1:0.75, Pre-Treatment</b>  | 2.254756        | 19.23493        | 27.88045        | 3.008616        | 6.61751         | 11.7992524 | 4.11953645 | -82%            |
| <b>1:0.75, Post-Treatment</b> | 3.758942        | 1.702527        | 2.916314        | 0.983693        | 1.389141        | 2.15012319 | 0.4209252  |                 |
| <b>1:0.50, Pre-Treatment</b>  | 2.711793        | 19.4545         | 26.14869        | 2.17238         | 3.636329        | 10.8247385 | 4.08922457 | -84%            |
| <b>1:0.50, Post-Treatment</b> | 4.045305        | 0.12529         | 3.252858        | 0.657387        | 0.627973        | 1.74176249 | 0.6485651  |                 |
| <b>1:0.25, Pre-Treatment</b>  | 2.969487        | 15.65505        | 30.38088        | 2.153999        | 3.984998        | 11.0288822 | 4.43183506 | -79%            |
| <b>1:0.25, Post-Treatment</b> | 4.254072        | 0.392017        | 4.497903        | 1.357452        | 0.939149        | 2.28811867 | 0.70779428 |                 |
| <b>0.75:1, Pre-Treatment</b>  | 1.971654        | 16.57457        | 25.37797        | 1.937486        | 2.851675        | 9.74267257 | 3.91549509 | -82%            |
| <b>0.75:1, Post-Treatment</b> | 3.626976        | -0.406965       | 3.753349        | 0.924049        | 0.844606        | 1.74840284 | 0.6755459  |                 |
| <b>0.50:1, Pre-Treatment</b>  | 2.441858        | 13.83865        | 20.13007        | 2.065923        | 3.087699        | 8.31283837 | 3.00541666 | -81%            |
| <b>0.50:1, Post-Treatment</b> | 3.049413        | 0.830298        | 2.641225        | 0.676077        | 0.838134        | 1.60702963 | 0.41678198 |                 |
| <b>0.25:1, Pre-Treatment</b>  | 1.692749        | 11.49924        | 13.10613        | 1.374271        | 2.676268        | 6.06973187 | 2.09532339 | -78%            |
| <b>0.25:1, Post-Treatment</b> | 2.644637        | 1.027387        | 2.019354        | 0.291877        | 0.693012        | 1.3352533  | 0.35488818 |                 |

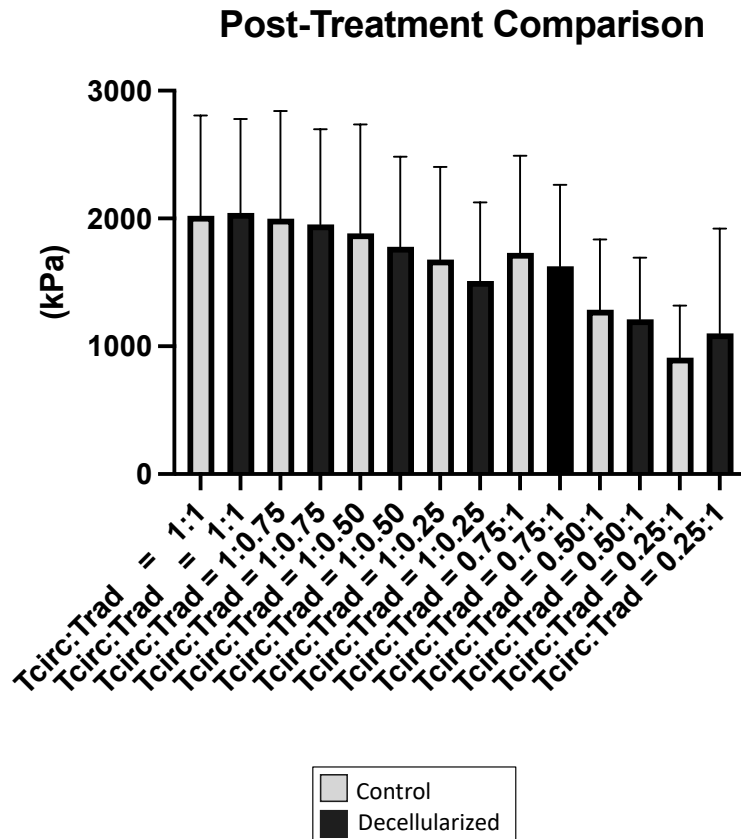
The same data analysis was performed for the high-tension modulus. For each of the seven loading ratios ( $T_{\text{circ}}:T_{\text{rad}} = 1:1, 1:0.75, 1:0.5, 1:0.25, 0.75:1, 0.5:1, 0.25:1$ ), the pre-treatment value and the post-treatment value for the high-tension modulus in the circumferential direction were compared to the using a paired  $t$  test. No statistically significant results were found from pre-treatment to post-treatment for any of the loading ratios, for either the control group or the decellularized group.



**Figure 5-9.** Circumferential high-tension modulus for control and decellularized treatment groups. Pre-treatment values are compared to post-treatment values with a paired  $t$  test.

Statistical significance is indicated with \* =  $p < 0.05$  , and \*\* =  $p < 0.005$ .

For the high-tension modulus in the circumferential direction, the post-treatment value for the control group was compared to the post-treatment value for the decellularized group for each loading protocol ( $T_{\text{circ}}:T_{\text{rad}} = 1:1, 1:0.75, 1:0.5, 1:0.25, 0.75:1, 0.5:1, 0.25:1$ ) using a paired  $t$  test. There were no statistically significant results from control group to decellularized group for any of the loading ratios (Figure 5-10).



**Figure 5-10.** Circumferential high-tension modulus post-treatment values from the control group are compared to the post-treatment values from the decellularized group with a paired  $t$  test.

Statistical significance is indicated with  $*$  =  $p < 0.05$  , and  $**$  =  $p < 0.005$ .

The circumferential high-tension modulus values were averaged and the percent change calculated between the pre-treatment and post-treatment values (Tables 5-6 and 5-7).

**Table 5-6.** Circumferential high-tension modulus values and % change from pre-treatment to post-treatment for the control group.

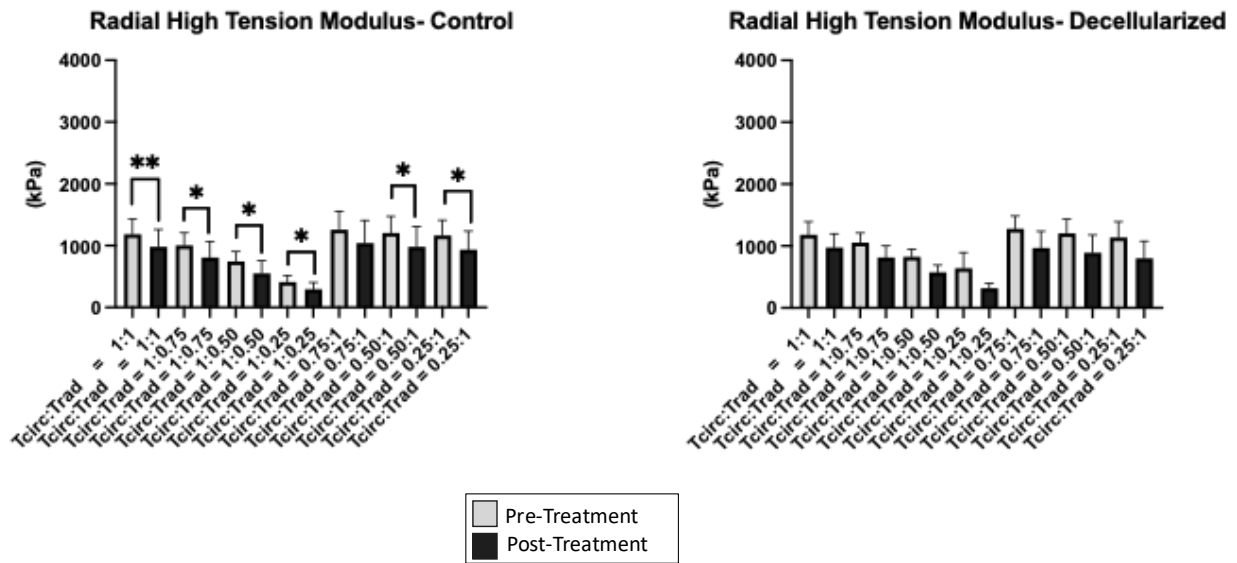
| <b>Control</b>                |                 |                 |                 |                 |                 |            |            |                 |
|-------------------------------|-----------------|-----------------|-----------------|-----------------|-----------------|------------|------------|-----------------|
|                               | <b>Tissue 1</b> | <b>Tissue 2</b> | <b>Tissue 3</b> | <b>Tissue 4</b> | <b>Tissue 5</b> | <b>AVG</b> | <b>SEM</b> | <b>% Change</b> |
| <b>1:1, Pre-Treatment</b>     | 1600.505        | 2034.399        | 3535.492        | 1835.955        | 2748.365        | 2350.94339 | 352.822135 | -14%            |
| <b>1:1, Post-Treatment</b>    | 650.2002        | 2113.654        | 2407.523        | 2355.739        | 2581.264        | 2021.67605 | 350.928808 |                 |
| <b>1:0.75, Pre-Treatment</b>  | 1563.936        | 2035.328        | 3319.377        | 1872.964        | 2931.832        | 2344.6876  | 333.358529 | -15%            |
| <b>1:0.75, Post-Treatment</b> | 521.5154        | 2087.959        | 2434.523        | 2437.4          | 2510.736        | 1998.42676 | 376.471903 |                 |
| <b>1:0.50, Pre-Treatment</b>  | 1505.511        | 1989.414        | 3036.578        | 1935.224        | 2976.1          | 2288.56566 | 304.937892 | -18%            |
| <b>1:0.50, Post-Treatment</b> | 392.299         | 1978.662        | 2330.672        | 2266.184        | 2453.731        | 1884.30954 | 381.07126  |                 |
| <b>1:0.25, Pre-Treatment</b>  | 1346.736        | 1825.068        | 2701.777        | 1871.68         | 2768.177        | 2102.68769 | 274.197313 | -20%            |
| <b>1:0.25, Post-Treatment</b> | 395.5036        | 1819.791        | 2021.42         | 2105.479        | 2052.007        | 1678.84017 | 324.457621 |                 |
| <b>0.75:1, Pre-Treatment</b>  | 1349.103        | 1655.018        | 3143.416        | 1643.934        | 2571.982        | 2072.69054 | 337.461493 | -17%            |
| <b>0.75:1, Post-Treatment</b> | 418.8434        | 1713.397        | 2247.735        | 2111.542        | 2160.071        | 1730.31778 | 340.440287 |                 |
| <b>0.50:1, Pre-Treatment</b>  | 1029.513        | 1241.275        | 2471.244        | 1175.96         | 1970.681        | 1577.73479 | 276.400251 | -18%            |
| <b>0.50:1, Post-Treatment</b> | 350.5541        | 1243.501        | 1649.023        | 1523.226        | 1663.416        | 1285.94404 | 245.699987 |                 |
| <b>0.25:1, Pre-Treatment</b>  | 794.1646        | 1172.822        | 2069.343        | 672.2816        | 1645.269        | 1270.77605 | 262.002186 | -28%            |
| <b>0.25:1, Post-Treatment</b> | 243.4143        | 1156.421        | 1019.139        | 856.9835        | 1285.487        | 912.289142 | 181.761753 |                 |

**Table 5-7.** Circumferential high-tension modulus values and % change from pre-treatment to post-treatment for the decellularized group.

| <b>Decellularized</b>         |                 |                 |                 |                 |                 |            |            |                 |
|-------------------------------|-----------------|-----------------|-----------------|-----------------|-----------------|------------|------------|-----------------|
|                               | <b>Tissue 1</b> | <b>Tissue 2</b> | <b>Tissue 3</b> | <b>Tissue 4</b> | <b>Tissue 5</b> | <b>AVG</b> | <b>SEM</b> | <b>% Change</b> |
| <b>1:1, Pre-Treatment</b>     | 1769.363        | 1246.673        | 1498.588        | 1997.276        | 2509.263        | 1804.23266 | 216.776543 | 13%             |
| <b>1:1, Post-Treatment</b>    | 888.9707        | 2127.876        | 1885.764        | 2823.8          | 2487.147        | 2042.71132 | 329.440816 |                 |
| <b>1:0.75, Pre-Treatment</b>  | 1716.604        | 1292.306        | 1597.968        | 1978.436        | 2495.594        | 1816.18144 | 202.473022 | 8%              |
| <b>1:0.75, Post-Treatment</b> | 791.1612        | 2111.71         | 1760.809        | 2767.403        | 2338.762        | 1953.96876 | 333.470746 |                 |
| <b>1:0.50, Pre-Treatment</b>  | 1680.137        | 1244.895        | 1455.98         | 1968.993        | 2271.259        | 1724.25277 | 182.045917 | 3%              |
| <b>1:0.50, Post-Treatment</b> | 679.0772        | 1839.644        | 1666.153        | 2577.533        | 2131.022        | 1778.68603 | 315.26307  |                 |
| <b>1:0.25, Pre-Treatment</b>  | 1503.708        | 1253.453        | 1531.901        | 2083.798        | 1978.651        | 1670.30213 | 156.001616 | -10%            |
| <b>1:0.25, Post-Treatment</b> | 532.8434        | 1595.211        | 1449.733        | 2200.396        | 1779.024        | 1511.44148 | 275.203419 |                 |
| <b>0.75:1, Pre-Treatment</b>  | 1618.264        | 1227.537        | 1524.879        | 1684.496        | 2404.49         | 1691.93318 | 194.52385  | -4%             |
| <b>0.75:1, Post-Treatment</b> | 651.4137        | 1662.46         | 1458.085        | 2306.314        | 2056.521        | 1626.95867 | 285.264238 |                 |
| <b>0.50:1, Pre-Treatment</b>  | 1208.333        | 937.6606        | 1322.65         | 1292.699        | 2077.317        | 1367.73192 | 189.939883 | -11%            |
| <b>0.50:1, Post-Treatment</b> | 463.6651        | 1201.207        | 1112.941        | 1655.47         | 1621.345        | 1210.92578 | 216.120048 |                 |
| <b>0.25:1, Pre-Treatment</b>  | 792.8888        | 856.2458        | 3789.622        | 1074.918        | 1830.887        | 1668.91239 | 561.440928 | -34%            |
| <b>0.25:1, Post-Treatment</b> | 277.736         | 714.9134        | 993.682         | 2455.843        | 1069.68         | 1102.37074 | 365.712573 |                 |

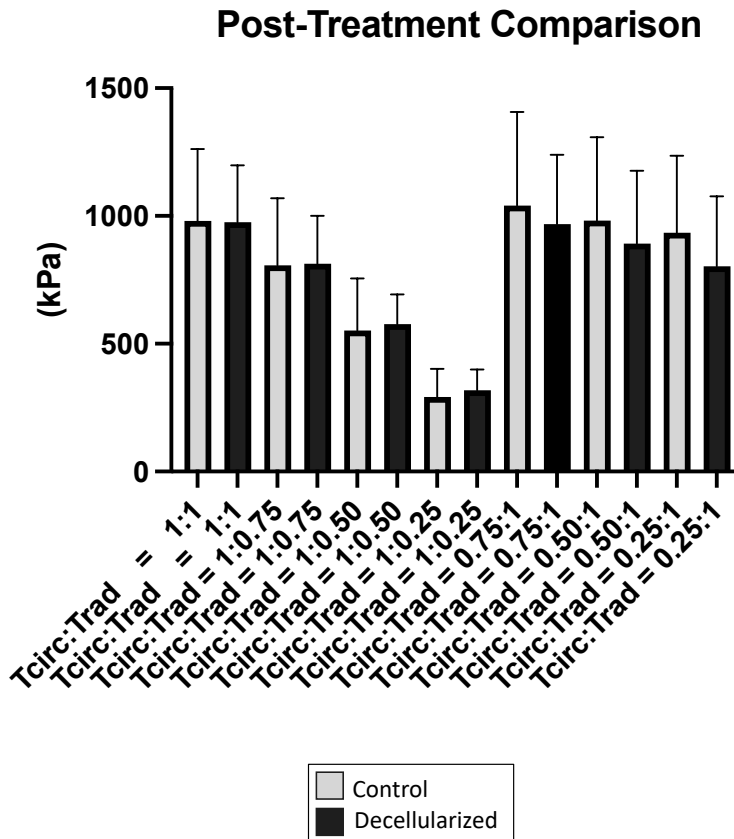


Finally, for each of the seven loading ratios ( $T_{\text{circ}}:T_{\text{rad}} = 1:1, 1:0.75, 1:0.5, 1:0.25, 0.75:1, 0.5:1, 0.25:1$ ), the pre-treatment value and the post-treatment value for the high-tension modulus in the radial direction were compared to the using a paired  $t$  test. No statistically significant results were found from pre-treatment to post-treatment for any of the loading ratios for the decellularized group. However, six out of seven loading ratios showed statistically significant results between pre-treatment and post-treatment values for the control group.



**Figure 5-11.** Radial high-tension modulus for control and decellularized treatment groups. Pre-treatment values are compared to post-treatment values with a paired  $t$  test. Statistical significance is indicated with  $*$  =  $p < 0.05$  , and  $**$  =  $p < 0.005$ .

For the high-tension modulus in the radial direction, the post-treatment value for the control group was compared to the post-treatment value for the decellularized group for each loading protocol ( $T_{\text{circ}}:T_{\text{rad}} = 1:1, 1:0.75, 1:0.5, 1:0.25, 0.75:1, 0.5:1, 0.25:1$ ) using a paired  $t$  test. There were no statistically significant results from control group to decellularized group for any of the loading ratios (Figure 5-12).



**Figure 5-12.** Radial high-tension modulus post-treatment values from the control group are compared to the post-treatment values from the decellularized group with a paired  $t$  test.

Statistical significance is indicated with \* =  $p < 0.05$  , and \*\* =  $p < 0.005$ .

The radial high-tension modulus values were averaged and the percent change calculated between the pre-treatment and post-treatment values (Tables 5-8 and 5-9).

**Table 5-8.** Radial high-tension modulus values and % change from pre-treatment to post-treatment for the control group.

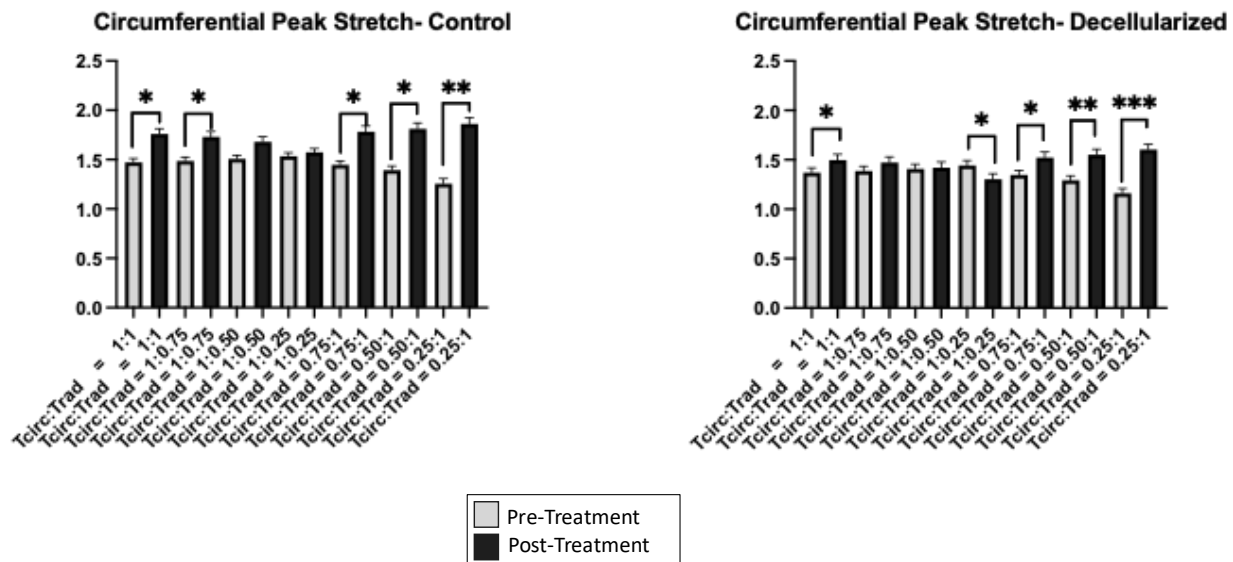
| <b>Control</b>                |                 |                 |                 |                 |                 |            |            |                 |
|-------------------------------|-----------------|-----------------|-----------------|-----------------|-----------------|------------|------------|-----------------|
|                               | <b>Tissue 1</b> | <b>Tissue 2</b> | <b>Tissue 3</b> | <b>Tissue 4</b> | <b>Tissue 5</b> | <b>AVG</b> | <b>SEM</b> | <b>% Change</b> |
| <b>1:1, Pre-Treatment</b>     | 855.1337        | 1176.131        | 1192.485        | 1552.92         | 1146.278        | 1184.58951 | 110.862508 |                 |
| <b>1:1, Post-Treatment</b>    | 560.946         | 1111.045        | 1019.167        | 1319.224        | 891.4622        | 980.368966 | 125.941295 | -17%            |
| <b>1:0.75, Pre-Treatment</b>  | 718.0962        | 1011.453        | 957.055         | 1278.618        | 1065.605        | 1006.16544 | 90.3291268 |                 |
| <b>1:0.75, Post-Treatment</b> | 400.0375        | 909.9954        | 901.6372        | 1094.778        | 728.5696        | 807.003452 | 117.079016 | -20%            |
| <b>1:0.50, Pre-Treatment</b>  | 516.7302        | 777.2989        | 667.9016        | 933.4453        | 834.3693        | 745.949056 | 71.6199917 |                 |
| <b>1:0.50, Post-Treatment</b> | 209.3183        | 616.8801        | 655.2747        | 733.0434        | 546.2275        | 552.14878  | 90.861369  | -26%            |
| <b>1:0.25, Pre-Treatment</b>  | 252.2736        | 424.2343        | 380.2116        | 542.5714        | 461.6754        | 412.193251 | 48.056755  |                 |
| <b>1:0.25, Post-Treatment</b> | 113.6512        | 327.3266        | 355.0693        | 394.1745        | 269.2279        | 291.889886 | 48.9857741 | -29%            |
| <b>0.75:1, Pre-Treatment</b>  | 842.7362        | 1186.164        | 1251.376        | 1676.555        | 1331.439        | 1257.65391 | 133.833715 |                 |
| <b>0.75:1, Post-Treatment</b> | 486.11          | 1168.062        | 1181.123        | 1460.525        | 908.8318        | 1040.93036 | 163.882817 | -17%            |
| <b>0.50:1, Pre-Treatment</b>  | 818.1853        | 1130.566        | 1241.825        | 1559.473        | 1281.543        | 1206.31846 | 120.004951 |                 |
| <b>0.50:1, Post-Treatment</b> | 514.2083        | 1045.008        | 1085.601        | 1402.348        | 864.5492        | 982.342947 | 145.605451 | -19%            |
| <b>0.25:1, Pre-Treatment</b>  | 813.839         | 1076.081        | 1143.039        | 1440.322        | 1351.87         | 1165.03014 | 110.0967   |                 |
| <b>0.25:1, Post-Treatment</b> | 538.5089        | 929.8122        | 987.4302        | 1375.006        | 840.103         | 934.172091 | 134.645532 | -20%            |

**Table 5-9.** Radial high-tension modulus values and % change from pre-treatment to post-treatment for the decellularized group.

| <b>Decellularized</b>         |                 |                 |                 |                 |                 |            |            |                 |
|-------------------------------|-----------------|-----------------|-----------------|-----------------|-----------------|------------|------------|-----------------|
|                               | <b>Tissue 1</b> | <b>Tissue 2</b> | <b>Tissue 3</b> | <b>Tissue 4</b> | <b>Tissue 5</b> | <b>AVG</b> | <b>SEM</b> | <b>% Change</b> |
| <b>1:1, Pre-Treatment</b>     | 1471.196        | 877.6081        | 1194.253        | 1207.869        | 1150.549        | 1180.295   | 94.361709  |                 |
| <b>1:1, Post-Treatment</b>    | 749.6117        | 1285.2          | 863.777         | 856.1671        | 1125.904        | 976.131895 | 99.0659223 | -17%            |
| <b>1:0.75, Pre-Treatment</b>  | 1224.634        | 816.425         | 1163.104        | 1044.896        | 1022.176        | 1054.24715 | 70.198587  |                 |
| <b>1:0.75, Post-Treatment</b> | 575.0392        | 1065.746        | 741.4478        | 764.7546        | 920.3737        | 813.47224  | 83.5108343 | -23%            |
| <b>1:0.50, Pre-Treatment</b>  | 943.3988        | 649.7565        | 929.7543        | 842.9613        | 757.6657        | 824.707311 | 55.0264047 |                 |
| <b>1:0.50, Post-Treatment</b> | 392.6014        | 689.8592        | 563.558         | 575.803         | 660.9619        | 576.5567   | 51.9474716 | -30%            |
| <b>1:0.25, Pre-Treatment</b>  | 559.4971        | 458.1954        | 1079.306        | 621.5601        | 497.0695        | 643.125578 | 112.526328 |                 |
| <b>1:0.25, Post-Treatment</b> | 178.578         | 368.8402        | 308.9111        | 360.7661        | 370.7191        | 317.562923 | 36.546617  | -51%            |
| <b>0.75:1, Pre-Treatment</b>  | 1564.972        | 1004.348        | 1323.636        | 1185.72         | 1317.725        | 1279.28003 | 92.0344102 |                 |
| <b>0.75:1, Post-Treatment</b> | 660.5202        | 1300.875        | 815.3935        | 859.8133        | 1202.037        | 967.727755 | 121.473349 | -24%            |
| <b>0.50:1, Pre-Treatment</b>  | 1503.242        | 902.6144        | 1206.994        | 1074.975        | 1332.146        | 1203.99421 | 103.309461 |                 |
| <b>0.50:1, Post-Treatment</b> | 601.1158        | 1213.981        | 750.0476        | 713.0022        | 1183.154        | 892.260162 | 127.523834 | -26%            |
| <b>0.25:1, Pre-Treatment</b>  | 1490.583        | 908.5355        | 1043.923        | 937.8293        | 1309.341        | 1138.04233 | 112.97012  |                 |
| <b>0.25:1, Post-Treatment</b> | 527.1352        | 1079.91         | 607.361         | 686.1639        | 1114.006        | 802.915245 | 122.766156 | -29%            |

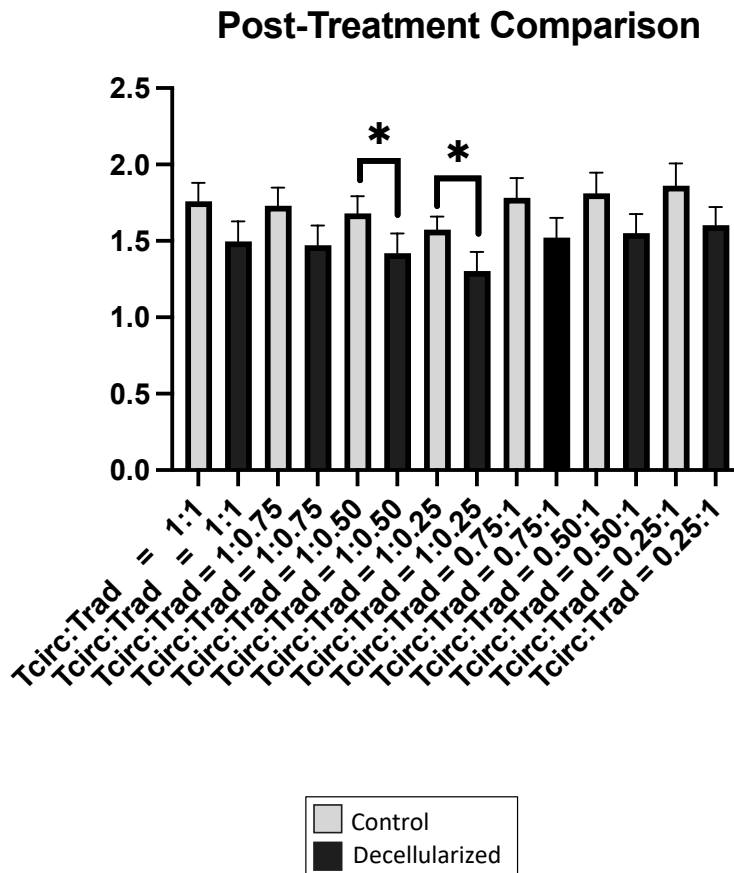
The peak tissue stretch, an approximate measure of overall tissue extensibility, was measured for each loading protocol in the circumferential and radial directions. This value was compared before and after treatment with a paired *t* test for both the control and decellularized groups.

In the circumferential direction, there is a general trend of higher extensibility post-treatment as compared to pre-treatment. However, these results are observed in both the control tissues as well as the decellularized tissues, indicating that this observation is most likely a result of the tissues soaking in solution for a week, rather than the decellularization treatment itself (Figure 5-13).



**Figure 5-13.** Peak stretch values for each loading protocol before treatment and after treatment in the circumferential direction. Statistical significance is indicated with \* =  $p < 0.05$  , and \*\* =  $p < 0.005$ .

For the peak stretch in the circumferential direction, the post-treatment value for the control group was compared to the post-treatment value for the decellularized group for each loading protocol ( $T_{\text{circ}}:T_{\text{rad}} = 1:1, 1:0.75, 1:0.5, 1:0.25, 0.75:1, 0.5:1, 0.25:1$ ) using a paired  $t$  test. Out of the seven loading ratios, two showed statistically significant results, with a decrease in the decellularized group as compared to the control group (Figure 5-14).



**Figure 5-14.** Circumferential peak stretch post-treatment values from the control group are compared to the post-treatment values from the decellularized group with a paired  $t$  test.

Statistical significance is indicated with \* =  $p < 0.05$  , and \*\* =  $p < 0.005$ .

The circumferential peak stretch values were averaged and the percent change calculated between the pre-treatment and post-treatment values (Tables 5-10 and 5-11).

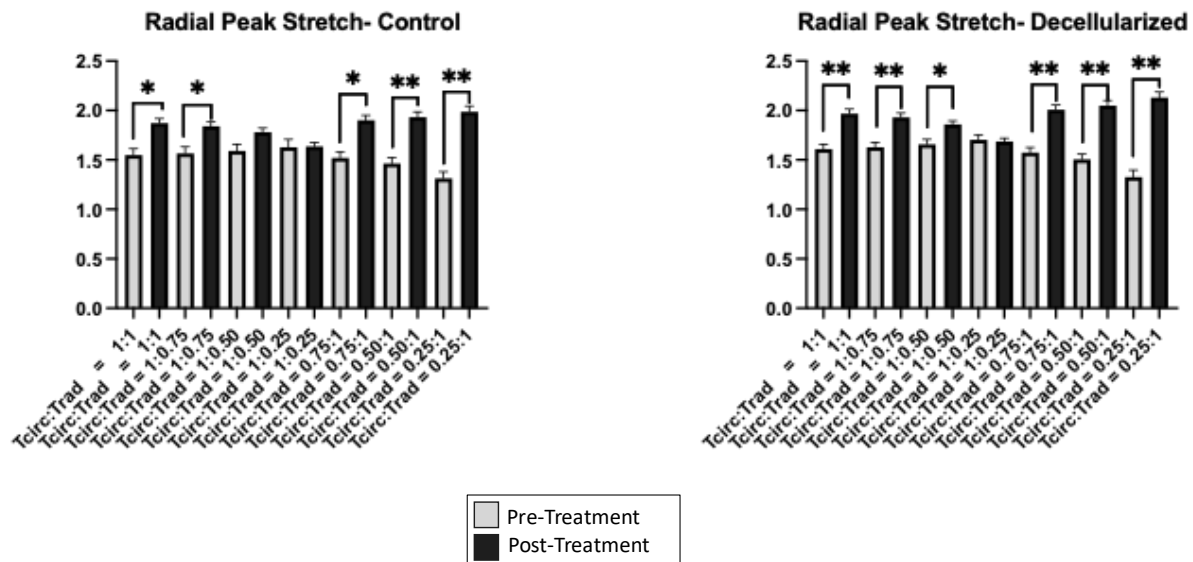
**Table 5-10.** Circumferential peak stretch values and % change from pre-treatment to post-treatment for the control group.

| <b>Control</b>                |                 |                 |                 |                 |                 |            |            |                 |
|-------------------------------|-----------------|-----------------|-----------------|-----------------|-----------------|------------|------------|-----------------|
|                               | <b>Tissue 1</b> | <b>Tissue 2</b> | <b>Tissue 3</b> | <b>Tissue 4</b> | <b>Tissue 5</b> | <b>AVG</b> | <b>SEM</b> | <b>% Change</b> |
| <b>1:1, Pre-Treatment</b>     | 1.4972          | 1.526197        | 1.347954        | 1.568591        | 1.423067        | 1.47260153 | 0.03916776 |                 |
| <b>1:1, Post-Treatment</b>    | 1.812958        | 1.7676          | 1.893081        | 1.560533        | 1.757899        | 1.7584143  | 0.05493253 | 19%             |
| <b>1:0.75, Pre-Treatment</b>  | 1.514133        | 1.545127        | 1.362352        | 1.578056        | 1.435333        | 1.48700039 | 0.03912345 |                 |
| <b>1:0.75, Post-Treatment</b> | 1.781362        | 1.7344          | 1.862952        | 1.54            | 1.735902        | 1.73092319 | 0.05313387 | 16%             |
| <b>1:0.50, Pre-Treatment</b>  | 1.537333        | 1.569657        | 1.383416        | 1.589788        | 1.452267        | 1.50649219 | 0.03870884 |                 |
| <b>1:0.50, Post-Treatment</b> | 1.72657         | 1.679067        | 1.811625        | 1.502667        | 1.683909        | 1.68076741 | 0.05047486 | 12%             |
| <b>1:0.25, Pre-Treatment</b>  | 1.5624          | 1.60312         | 1.421944        | 1.604986        | 1.4756          | 1.53360987 | 0.03646196 |                 |
| <b>1:0.25, Post-Treatment</b> | 1.634849        | 1.564533        | 1.650847        | 1.4324          | 1.584722        | 1.57347012 | 0.03864045 | 3%              |
| <b>0.75:1, Pre-Treatment</b>  | 1.469333        | 1.488202        | 1.323557        | 1.553793        | 1.396933        | 1.44636359 | 0.03958782 |                 |
| <b>0.75:1, Post-Treatment</b> | 1.833089        | 1.7996          | 1.917211        | 1.571867        | 1.791628        | 1.78267888 | 0.05720501 | 23%             |
| <b>0.50:1, Pre-Treatment</b>  | 1.409467        | 1.411812        | 1.273164        | 1.525397        | 1.348           | 1.39356772 | 0.04155602 |                 |
| <b>0.50:1, Post-Treatment</b> | 1.867084        | 1.836667        | 1.948407        | 1.586667        | 1.820157        | 1.81179638 | 0.06045288 | 30%             |
| <b>0.25:1, Pre-Treatment</b>  | 1.25            | 1.194374        | 1.156779        | 1.455006        | 1.218267        | 1.25488517 | 0.052297   |                 |
| <b>0.25:1, Post-Treatment</b> | 1.923077        | 1.899467        | 1.9972          | 1.615867        | 1.874817        | 1.86208546 | 0.06486876 | 48%             |

**Table 5-11.** Circumferential peak stretch values and % change from pre-treatment to post-treatment for the decellularized group.

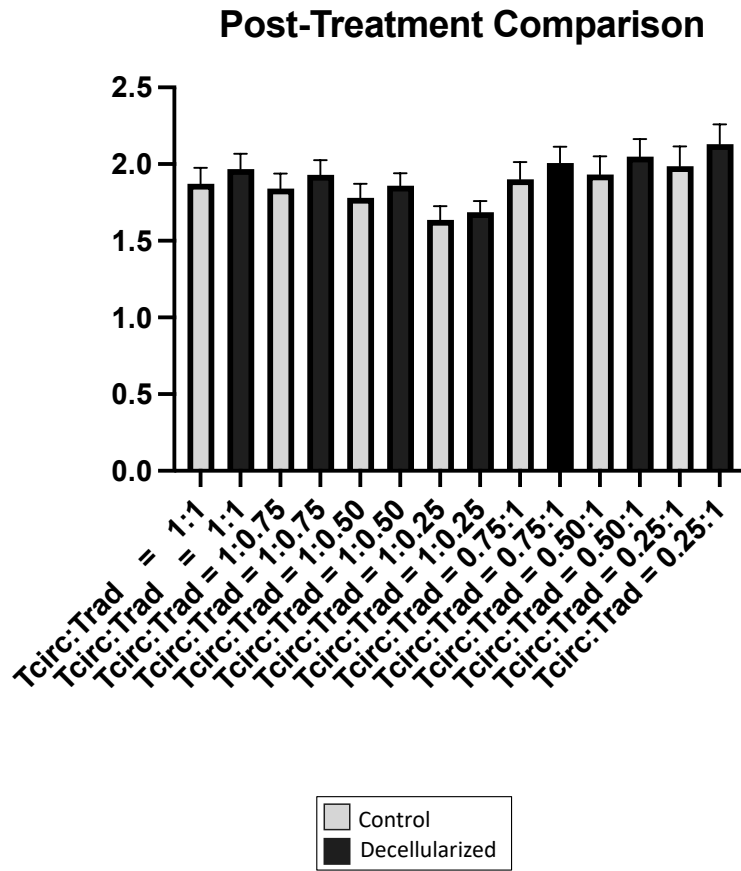
| <b>Decellularized</b>         |                 |                 |                 |                 |                 |            |            |                 |
|-------------------------------|-----------------|-----------------|-----------------|-----------------|-----------------|------------|------------|-----------------|
|                               | <b>Tissue 1</b> | <b>Tissue 2</b> | <b>Tissue 3</b> | <b>Tissue 4</b> | <b>Tissue 5</b> | <b>AVG</b> | <b>SEM</b> | <b>% Change</b> |
| <b>1:1, Pre-Treatment</b>     | 1.526996        | 1.336533        | 1.272533        | 1.420933        | 1.294894        | 1.37037808 | 0.04663799 |                 |
| <b>1:1, Post-Treatment</b>    | 1.622317        | 1.433809        | 1.296627        | 1.5724          | 1.554993        | 1.49602913 | 0.05869002 | 9%              |
| <b>1:0.75, Pre-Treatment</b>  | 1.541528        | 1.3528          | 1.290133        | 1.4408          | 1.308492        | 1.38675067 | 0.04663112 |                 |
| <b>1:0.75, Post-Treatment</b> | 1.59832         | 1.413145        | 1.271697        | 1.536533        | 1.536862        | 1.47131147 | 0.05827143 | 6%              |
| <b>1:0.50, Pre-Treatment</b>  | 1.565391        | 1.3708          | 1.3088          | 1.465467        | 1.327956        | 1.40768284 | 0.0478045  |                 |
| <b>1:0.50, Post-Treatment</b> | 1.556193        | 1.369551        | 1.222637        | 1.468267        | 1.485802        | 1.42048976 | 0.05775121 | 1%              |
| <b>1:0.25, Pre-Treatment</b>  | 1.614985        | 1.401333        | 1.340667        | 1.4944          | 1.361818        | 1.44264062 | 0.05050679 |                 |
| <b>1:0.25, Post-Treatment</b> | 1.411012        | 1.282762        | 1.09772         | 1.357067        | 1.368884        | 1.30348906 | 0.05544304 | -10%            |
| <b>0.75:1, Pre-Treatment</b>  | 1.507266        | 1.315467        | 1.254           | 1.388133        | 1.268631        | 1.34669931 | 0.04645518 |                 |
| <b>0.75:1, Post-Treatment</b> | 1.639515        | 1.461272        | 1.324223        | 1.600133        | 1.582322        | 1.52149314 | 0.05760014 | 13%             |
| <b>0.50:1, Pre-Treatment</b>  | 1.455539        | 1.267333        | 1.192           | 1.319467        | 1.22717         | 1.29230179 | 0.04599482 |                 |
| <b>0.50:1, Post-Treatment</b> | 1.665645        | 1.489935        | 1.363152        | 1.635733        | 1.604586        | 1.55181004 | 0.05577065 | 20%             |
| <b>0.25:1, Pre-Treatment</b>  | 1.32609         | 1.156667        | 1.029733        | 1.160267        | 1.132116        | 1.16097445 | 0.04761261 |                 |
| <b>0.25:1, Post-Treatment</b> | 1.713905        | 1.534329        | 1.432742        | 1.694533        | 1.642581        | 1.60361804 | 0.0528897  | 38%             |

The same general trend of higher extensibility post-treatment as compared to pre-treatment was observed in the radial direction as well. Once again, these results are observed in both the control tissues as well as the decellularized tissues, indicating that this observation is most likely a result of the tissues soaking in solution for a week, rather than the decellularization treatment itself (Figure 5-15).



**Figure 5-15.** Peak stretch values for each loading protocol before treatment and after treatment in the radial direction. Statistical significance is indicated with \* =  $p < 0.05$  , and \*\* =  $p < 0.005$ .

For the peak stretch in the radial direction, the post-treatment value for the control group was compared to the post-treatment value for the decellularized group for each loading protocol ( $T_{\text{circ}}:T_{\text{rad}} = 1:1, 1:0.75, 1:0.5, 1:0.25, 0.75:1, 0.5:1, 0.25:1$ ) using a paired  $t$  test. None of the loading ratios showed statistically significant results (Figure 5-14).



**Figure 5-16.** Radial peak stretch post-treatment values from the control group are compared to the post-treatment values from the decellularized group with a paired  $t$  test. Statistical significance is indicated with \* =  $p < 0.05$  , and \*\* =  $p < 0.005$ .



The radial peak stretch values were averaged and the percent change calculated between the pre-treatment and post-treatment values (Tables 5-12 and 5-13).

**Table 5-12.** Radial peak stretch values and % change from pre-treatment to post-treatment for the control group.

| <b>Control</b>                |          |          |          |          |          |            |            |          |
|-------------------------------|----------|----------|----------|----------|----------|------------|------------|----------|
|                               | Tissue 1 | Tissue 2 | Tissue 3 | Tissue 4 | Tissue 5 | AVG        | SEM        | % Change |
| <b>1:1, Pre-Treatment</b>     | 1.799385 | 1.532995 | 1.46639  | 1.515538 | 1.433077 | 1.54947694 | 0.06493449 |          |
| <b>1:1, Post-Treatment</b>    | 1.8994   | 1.864154 | 1.814308 | 1.749885 | 2.030611 | 1.87167139 | 0.04701579 | 21%      |
| <b>1:0.75, Pre-Treatment</b>  | 1.822308 | 1.549608 | 1.480541 | 1.524    | 1.454615 | 1.56621446 | 0.06611951 |          |
| <b>1:0.75, Post-Treatment</b> | 1.860483 | 1.831231 | 1.790769 | 1.727427 | 1.991386 | 1.8402591  | 0.04388067 | 17%      |
| <b>1:0.50, Pre-Treatment</b>  | 1.863077 | 1.572681 | 1.502692 | 1.535077 | 1.476154 | 1.58993614 | 0.07016806 |          |
| <b>1:0.50, Post-Treatment</b> | 1.784187 | 1.775385 | 1.726923 | 1.688202 | 1.927703 | 1.78048    | 0.04068049 | 12%      |
| <b>1:0.25, Pre-Treatment</b>  | 1.939077 | 1.607906 | 1.534995 | 1.550923 | 1.504462 | 1.62747253 | 0.07969436 |          |
| <b>1:0.25, Post-Treatment</b> | 1.57868  | 1.634923 | 1.566308 | 1.611137 | 1.789878 | 1.63618524 | 0.04027427 | 1%       |
| <b>0.75:1, Pre-Treatment</b>  | 1.761077 | 1.494385 | 1.438394 | 1.499231 | 1.403231 | 1.51926361 | 0.06304658 |          |
| <b>0.75:1, Post-Treatment</b> | 1.932164 | 1.895692 | 1.850615 | 1.762344 | 2.06722  | 1.90160733 | 0.05019502 | 25%      |
| <b>0.50:1, Pre-Treatment</b>  | 1.691077 | 1.422089 | 1.391324 | 1.471231 | 1.344154 | 1.46397497 | 0.06042251 |          |
| <b>0.50:1, Post-Treatment</b> | 1.974004 | 1.930154 | 1.882308 | 1.775573 | 2.099369 | 1.93228157 | 0.05325344 | 32%      |
| <b>0.25:1, Pre-Treatment</b>  | 1.539231 | 1.195662 | 1.265805 | 1.390154 | 1.173385 | 1.31284734 | 0.06805179 |          |
| <b>0.25:1, Post-Treatment</b> | 2.029534 | 2.003077 | 1.943385 | 1.803415 | 2.154745 | 1.98683115 | 0.05736366 | 51%      |

**Table 5-13.** Radial peak stretch values and % change from pre-treatment to post-treatment for the decellularized group.

| <b>Decellularized</b>         |          |          |          |          |          |            |            |          |
|-------------------------------|----------|----------|----------|----------|----------|------------|------------|----------|
|                               | Tissue 1 | Tissue 2 | Tissue 3 | Tissue 4 | Tissue 5 | AVG        | SEM        | % Change |
| <b>1:1, Pre-Treatment</b>     | 1.733579 | 1.631749 | 1.621443 | 1.426242 | 1.632672 | 1.60913706 | 0.05007649 |          |
| <b>1:1, Post-Treatment</b>    | 1.929088 | 1.836487 | 2.03261  | 1.948    | 2.095231 | 1.96828313 | 0.04448127 | 22%      |
| <b>1:0.75, Pre-Treatment</b>  | 1.758191 | 1.645593 | 1.64267  | 1.44747  | 1.650054 | 1.62879557 | 0.05027368 |          |
| <b>1:0.75, Post-Treatment</b> | 1.898016 | 1.808952 | 1.986464 | 1.9      | 2.058462 | 1.93037866 | 0.04258244 | 19%      |
| <b>1:0.50, Pre-Treatment</b>  | 1.786802 | 1.663129 | 1.675435 | 1.481157 | 1.683126 | 1.65792955 | 0.04940903 |          |
| <b>1:0.50, Post-Treatment</b> | 1.848331 | 1.76219  | 1.903861 | 1.808308 | 1.970769 | 1.85869187 | 0.03644175 | 12%      |
| <b>1:0.25, Pre-Treatment</b>  | 1.839255 | 1.695893 | 1.720966 | 1.526842 | 1.734502 | 1.70349177 | 0.05047855 |          |
| <b>1:0.25, Post-Treatment</b> | 1.736656 | 1.62252  | 1.727734 | 1.589692 | 1.751846 | 1.68568963 | 0.03312697 | -1%      |
| <b>0.75:1, Pre-Treatment</b>  | 1.706199 | 1.609599 | 1.570835 | 1.383787 | 1.595754 | 1.57323489 | 0.05263323 |          |
| <b>0.75:1, Post-Treatment</b> | 1.951238 | 1.858329 | 2.083526 | 2.007231 | 2.131077 | 2.00628021 | 0.04819803 | 28%      |
| <b>0.50:1, Pre-Treatment</b>  | 1.633287 | 1.559914 | 1.477311 | 1.315028 | 1.53884  | 1.50487617 | 0.05360694 |          |
| <b>0.50:1, Post-Treatment</b> | 1.989079 | 1.889709 | 2.143363 | 2.062615 | 2.165231 | 2.04999932 | 0.05077321 | 36%      |
| <b>0.25:1, Pre-Treatment</b>  | 1.485771 | 1.421935 | 1.214429 | 1.106138 | 1.401784 | 1.32601138 | 0.07115526 |          |
| <b>0.25:1, Post-Treatment</b> | 2.034918 | 1.954622 | 2.258268 | 2.167231 | 2.231077 | 2.12922314 | 0.05824529 | 61%      |

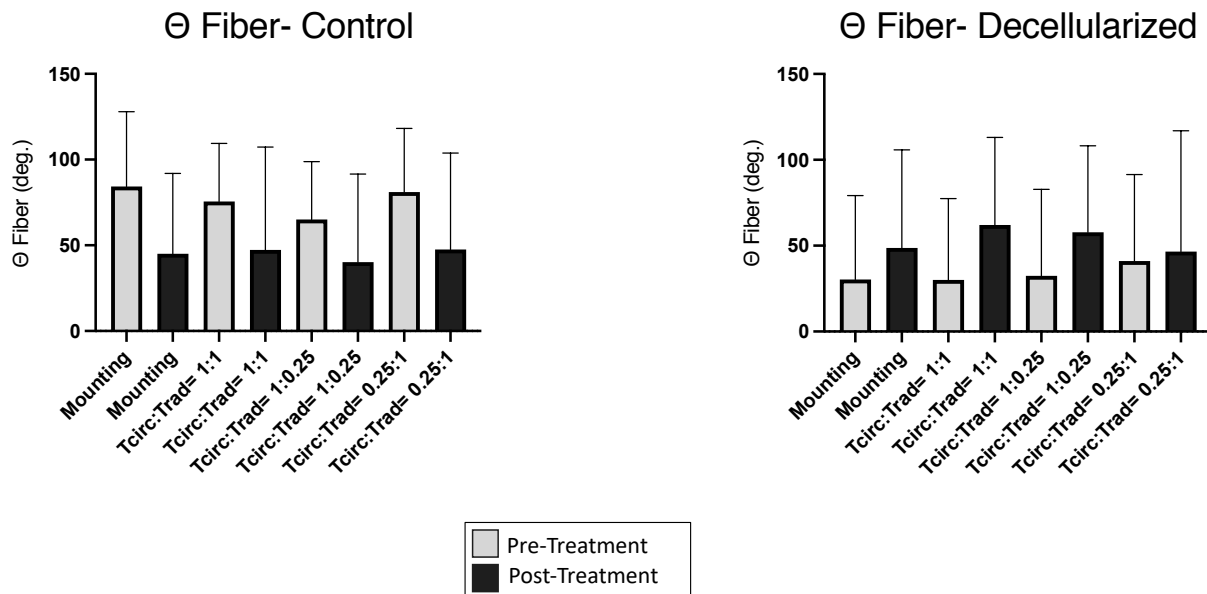
A one-way multivariate analysis of variance (MANOVA) was used to determine if there are any differences between decellularized and control groups for six dependent variables (circumferential high tension modulus, radial high tension modulus, circumferential low tension modulus, radial low tension modulus, circumferential peak stretch, and radial peak stretch). In this study, the independent variable is treatment, which has two groups of decellularized and control. This one-way MANOVA test was repeated for each loading ratio ( $T_{\text{circ}}:T_{\text{rad}} = 1:1, 1:0.75, 1:0.5, 1:0.25, 0.75:1, 0.5:1, 0.25:1$ ). There were no statistically significant results for any of the loading ratios, so no post-hoc analysis was attempted (Table 5-14).

**Table 5-14.** *P*-value results from one-way MANOVA repeated for each loading protocol.

| <b>Tcirc:Trad</b> | <b>P Value</b> | <b>Significance</b> |
|-------------------|----------------|---------------------|
| 1:1               | 0.54           | n.s.                |
| 1:0.75            | 0.56           | n.s.                |
| 1:0.5             | 0.52           | n.s.                |
| 1:0.25            | 0.44           | n.s.                |
| 0.75:1            | 0.42           | n.s.                |
| 0.5:1             | 0.53           | n.s.                |
| 0.25:1            | 0.35           | n.s.                |

### 5.3 Results- pSFDI Analysis

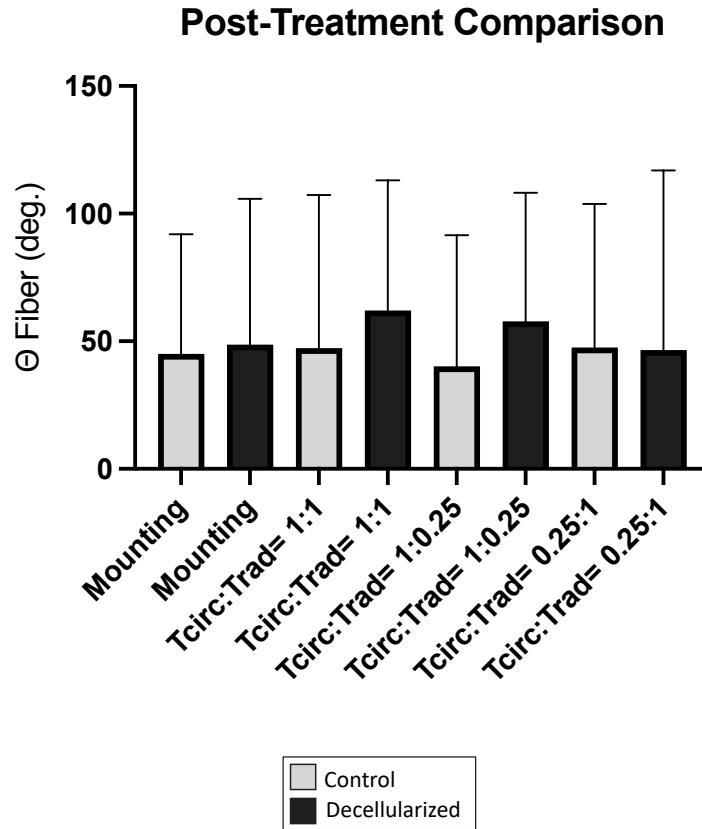
pSFDI analysis was performed with the tissue in four biaxial loading ratios ( $T_{\text{circ}}:T_{\text{rad}} =$  mounting, 1:1, 1:0.25, 0.25:1). In order to determine if the decellularization treatment influences average  $\theta_{\text{Fiber}}$  across the leaflet, pre-treatment  $\theta_{\text{Fiber}}$  values were compared to post-treatment  $\theta_{\text{Fiber}}$  values for each loading protocol for both the control and decellularized groups using a paired  $t$  test. No statistically significant results were found from pre-treatment to post-treatment for any of the loading ratios, in either the control group or the decellularized group (Figure 5-17).



**Figure 5-17.**  $\theta_{\text{Fiber}}$  values for each loading protocol before treatment and after treatment.

Statistical significance is indicated with \* =  $p < 0.05$  , and \*\* =  $p < 0.005$ .

Post-treatment  $\theta_{\text{Fiber}}$  values for the control group were also compared to post-treatment  $\theta_{\text{Fiber}}$  values for the decellularized group with a paired  $t$  test. No statistically significant results were found from the control group to the decellularized group for any of the loading ratios.



**Figure 5-18.**  $\theta_{\text{Fiber}}$  post-treatment values from the control group are compared to the post-treatment values from the decellularized group with a paired  $t$  test. Statistical significance is indicated with \* =  $p < 0.05$  , and \*\* =  $p < 0.005$ .

The  $\theta_{\text{Fiber}}$  values were averaged and the percent change calculated between the pre-treatment and post-treatment values (Tables 5-14 and 5-15).

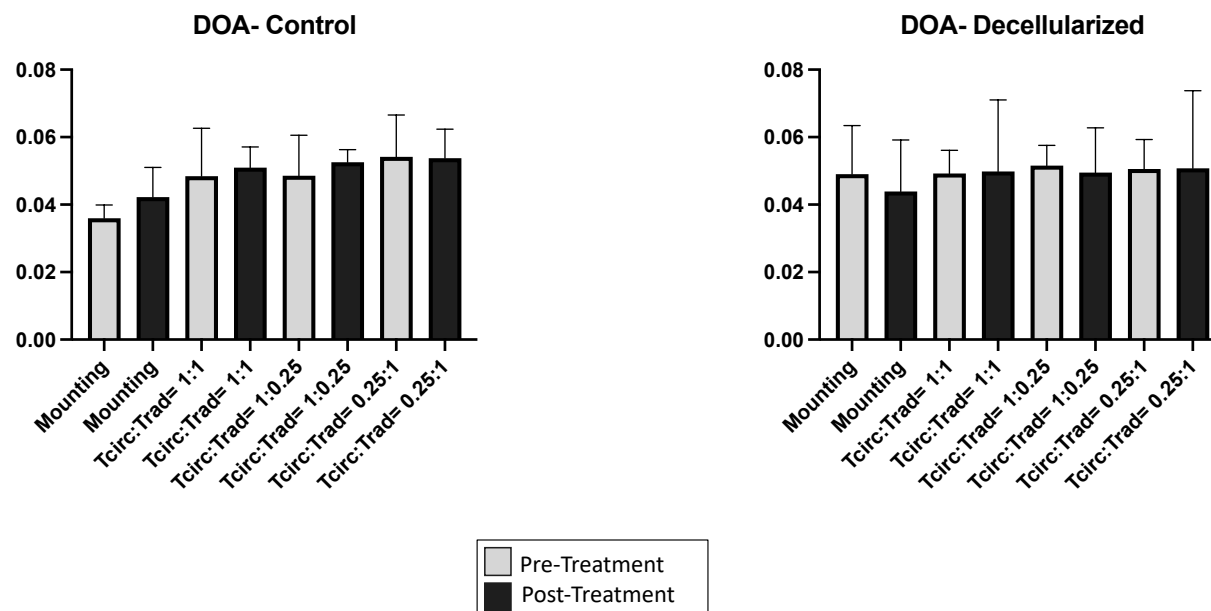
**Table 5-15.**  $\theta_{\text{Fiber}}$  values and % change from pre-treatment to post-treatment for the control group.

| <b>Control</b>                  |                 |                 |                 |                 |                 |             |            |                 |
|---------------------------------|-----------------|-----------------|-----------------|-----------------|-----------------|-------------|------------|-----------------|
|                                 | <b>Tissue 1</b> | <b>Tissue 2</b> | <b>Tissue 3</b> | <b>Tissue 4</b> | <b>Tissue 5</b> | <b>AVG</b>  | <b>SEM</b> | <b>% Change</b> |
| <b>Mounting, Pre-Treatment</b>  | 7.72690043      | 102.448364      | 94.120553       | 117.298228      | 100.029436      | 84.32469623 | 19.526317  | 8%              |
| <b>Mounting, Post-Treatment</b> | 111.428554      | 12.9706619      | -4.1096435      | 31.7353753      | 73.1531006      | 45.0356097  | 20.9987254 |                 |
| <b>1:1, Pre-Treatment</b>       | 15.9797076      | 87.2551034      | 97.2726243      | 81.4604726      | 95.7071125      | 75.5350041  | 15.1636792 | 77%             |
| <b>1:1, Post-Treatment</b>      | 114.328553      | 2.58821309      | 10.7497533      | -2.4510351      | 111.192331      | 47.28156302 | 26.8191024 |                 |
| <b>0.25:1, Pre-Treatment</b>    | 15.3345513      | 95.8750082      | 91.2395383      | 98.0442103      | 104.832388      | 81.06513926 | 16.5778946 | 52%             |
| <b>0.25:1, Post-Treatment</b>   | 119.790476      | 27.3200318      | -22.837197      | 26.2819908      | 87.4127945      | 47.59361924 | 25.1233524 |                 |
| <b>1:0.25, Pre-Treatment</b>    | 7.15535757      | 74.2914284      | 93.4078004      | 81.7910858      | 68.9453327      | 65.11820096 | 15.0611633 | 52%             |
| <b>1:0.25, Post-Treatment</b>   | 74.6995816      | -15.070983      | 29.0610432      | 2.86264467      | 109.358017      | 40.18206075 | 22.9631082 |                 |

**Table 5-16.**  $\theta_{\text{Fiber}}$  values and % Change from pre-treatment to post-treatment for the decellularized group.

| <b>Decellularized</b>           |                 |                 |                 |                 |                 |             |            |                 |
|---------------------------------|-----------------|-----------------|-----------------|-----------------|-----------------|-------------|------------|-----------------|
|                                 | <b>Tissue 1</b> | <b>Tissue 2</b> | <b>Tissue 3</b> | <b>Tissue 4</b> | <b>Tissue 5</b> | <b>AVG</b>  | <b>SEM</b> | <b>% Change</b> |
| <b>Mounting, Pre-Treatment</b>  | 36.8254825      | 61.8716611      | -17.666057      | -20.173485      | 90.7955841      | 30.33063719 | 21.8487734 | 17%             |
| <b>Mounting, Post-Treatment</b> | -37.625086      | 62.4201779      | 105.574309      | 88.3974258      | 24.9252988      | 48.7384251  | 25.5108462 |                 |
| <b>1:1, Pre-Treatment</b>       | -8.2422616      | 68.1232655      | -18.334127      | 18.6238411      | 89.964606       | 30.02706473 | 21.1863271 | 8%              |
| <b>1:1, Post-Treatment</b>      | -20.09817       | 109.392589      | 94.3165506      | 77.1588753      | 49.4266256      | 62.03929402 | 22.823672  |                 |
| <b>0.25:1, Pre-Treatment</b>    | -8.5290893      | 109.122431      | 6.76790905      | 19.0719978      | 78.6806976      | 41.0227892  | 22.5458444 | 40%             |
| <b>0.25:1, Post-Treatment</b>   | -27.955541      | 98.9243973      | 85.6045287      | 108.179066      | -32.134298      | 46.52363065 | 31.47123   |                 |
| <b>1:0.25, Pre-Treatment</b>    | 20.6540158      | 58.091728       | -32.377548      | 13.7470809      | 101.943133      | 32.41168196 | 22.5591909 | 0%              |
| <b>1:0.25, Post-Treatment</b>   | 32.8507327      | 79.5738241      | 91.1058112      | 104.018142      | -18.638661      | 57.78196995 | 22.5663757 |                 |

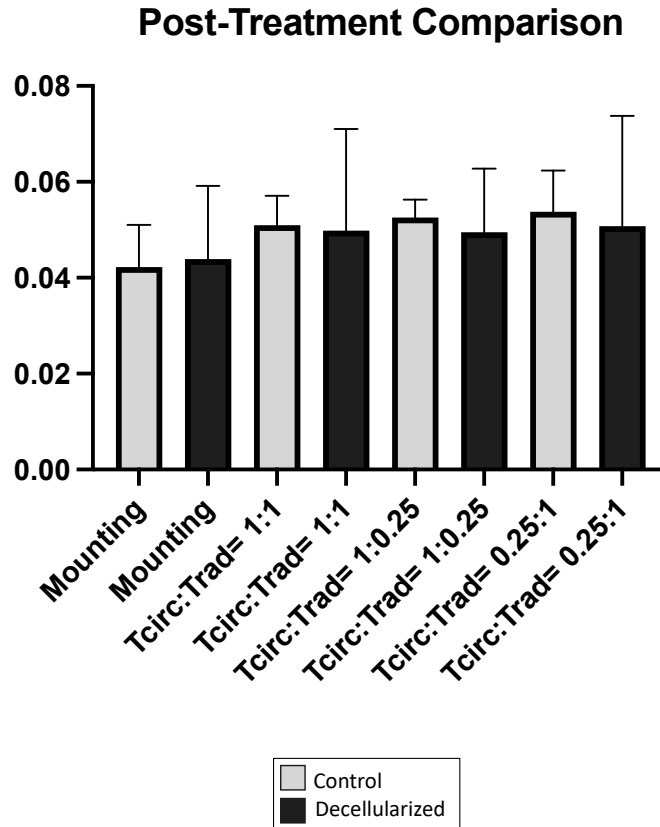
Pre-treatment DOA values were compared to post-treatment DOA values for each loading protocol for both the control and decellularized groups using a paired t test. No statistically significant results were found from pre-treatment to post-treatment for any of the loading ratios, in either the control group or the decellularized group (Figure 5-19).



**Figure 5-19.** DOA values for each loading protocol before treatment and after treatment.

Statistical significance is indicated with \* =  $p < 0.05$  , and \*\* =  $p < 0.005$ .

Post-treatment DOA values for the control group were also compared to post-treatment DOA values for the decellularized group with a paired *t* test. No statistically significant results were found from the control group to the decellularized group for any of the loading ratios.



**Figure 5-20.** DOA post-treatment values from the control group are compared to the post-treatment values from the decellularized group with a paired *t* test. Statistical significance is indicated with \* =  $p < 0.05$ , and \*\* =  $p < 0.005$ .

The DOA values were averaged and the percent change calculated between the pre-treatment and post-treatment values (Tables 5-16 and 5-17).

**Table 5-17.** DOA values and % change from pre-treatment to post-treatment for the control group.

| <b>Control</b>                  |                 |                 |                 |                 |                 |                   |                   |                 |
|---------------------------------|-----------------|-----------------|-----------------|-----------------|-----------------|-------------------|-------------------|-----------------|
|                                 | <b>Tissue 1</b> | <b>Tissue 2</b> | <b>Tissue 3</b> | <b>Tissue 4</b> | <b>Tissue 5</b> | <b>AVG</b>        | <b>SEM</b>        | <b>% Change</b> |
| <b>Mounting, Pre-Treatment</b>  | 0.04286324      | 0.03395346      | 0.03535408      | 0.03398238      | 0.03365006      | <b>0.03596064</b> | <b>0.00175064</b> | 125%            |
| <b>Mounting, Post-Treatment</b> | 0.05399599      | 0.0487546       | 0.03687108      | 0.03285801      | 0.03852988      | <b>0.04220191</b> | <b>0.00394492</b> |                 |
| <b>1:1, Pre-Treatment</b>       | 0.06132054      | 0.06062569      | 0.0390142       | 0.05244398      | 0.02871334      | <b>0.04842355</b> | <b>0.00635774</b> | -57%            |
| <b>1:1, Post-Treatment</b>      | 0.06143713      | 0.0508745       | 0.0456644       | 0.04855617      | 0.04819562      | <b>0.05094556</b> | <b>0.00274991</b> |                 |
| <b>0.25:1, Pre-Treatment</b>    | 0.07029164      | 0.06361584      | 0.04441236      | 0.05117472      | 0.04127906      | <b>0.05415472</b> | <b>0.00556547</b> | -31%            |
| <b>0.25:1, Post-Treatment</b>   | 0.0611084       | 0.06361766      | 0.04286106      | 0.05257408      | 0.04858284      | <b>0.05374881</b> | <b>0.00386114</b> |                 |
| <b>1:0.25, Pre-Treatment</b>    | 0.05310294      | 0.06373774      | 0.04921365      | 0.04613976      | 0.03066327      | <b>0.04857147</b> | <b>0.00537391</b> | -69%            |
| <b>1:0.25, Post-Treatment</b>   | 0.05481477      | 0.05478718      | 0.05393153      | 0.04601705      | 0.05333598      | <b>0.0525773</b>  | <b>0.00166337</b> |                 |

**Table 5-18.** DOA values and % change from pre-treatment to post-treatment for the decellularized group.

| <b>Decellularized</b>           |                 |                 |                 |                 |                 |            |            |                 |
|---------------------------------|-----------------|-----------------|-----------------|-----------------|-----------------|------------|------------|-----------------|
|                                 | <b>Tissue 1</b> | <b>Tissue 2</b> | <b>Tissue 3</b> | <b>Tissue 4</b> | <b>Tissue 5</b> | <b>AVG</b> | <b>SEM</b> | <b>% Change</b> |
| <b>Mounting, Pre-Treatment</b>  | 0.06464886      | 0.04363585      | 0.06413646      | 0.03784592      | 0.03485073      | 0.04902356 | 0.0064319  | 6%              |
| <b>Mounting, Post-Treatment</b> | 0.06550218      | 0.05377333      | 0.03242236      | 0.02974766      | 0.03821248      | 0.0439316  | 0.00681361 |                 |
| <b>1:1, Pre-Treatment</b>       | 0.05729272      | 0.03969912      | 0.04600949      | 0.05402215      | 0.04922376      | 0.04924945 | 0.00307555 | 208%            |
| <b>1:1, Post-Treatment</b>      | 0.05027225      | 0.06279526      | 0.030822        | 0.02772111      | 0.0776501       | 0.04985215 | 0.00946667 |                 |
| <b>0.25:1, Pre-Treatment</b>    | 0.0598802       | 0.04484218      | 0.0389325       | 0.05196502      | 0.05736431      | 0.05059684 | 0.00389246 | 164%            |
| <b>0.25:1, Post-Treatment</b>   | 0.05935833      | 0.0669326       | 0.02379512      | 0.02894497      | 0.07472763      | 0.05075173 | 0.01027845 |                 |
| <b>1:0.25, Pre-Treatment</b>    | 0.06026112      | 0.04410218      | 0.05270133      | 0.05260829      | 0.04813489      | 0.05156156 | 0.00269686 | 120%            |
| <b>1:0.25, Post-Treatment</b>   | 0.0576494       | 0.06005227      | 0.03484131      | 0.03517921      | 0.05971897      | 0.04948823 | 0.00592517 |                 |

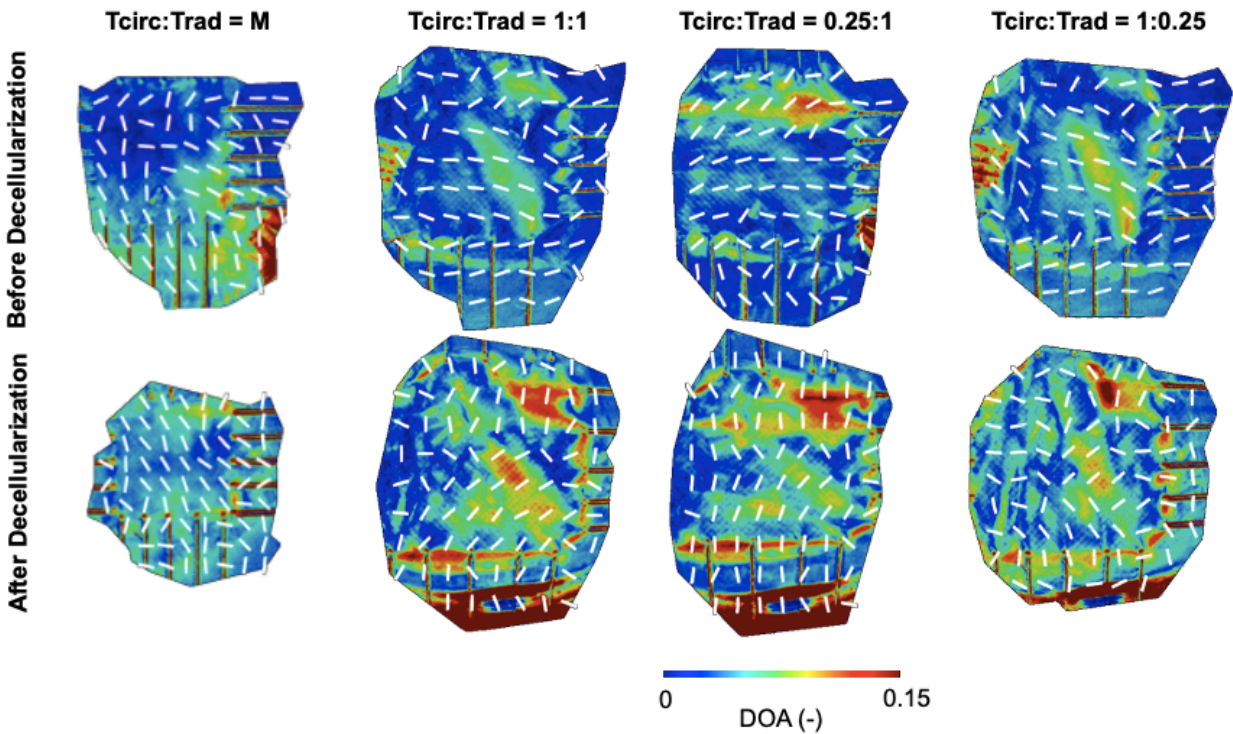


A one-way MANOVA was used to determine if there are any differences between decellularized and control groups for two dependent variables ( $\theta_{\text{Fiber}}$  and DOA). In this study, the independent variable is treatment, which has two groups of decellularized and control. This one-way MANOVA test was repeated for each loading ratio ( $T_{\text{circ}}:T_{\text{rad}} = \text{mounting}, 1:1, 1:0.25, 0.25:1$ ). There were no statistically significant results for any of the loading ratios, so no post-hoc analysis was attempted (Table 5-19).

**Table 5-19.** *P*-value results from one-way MANOVA repeated for each loading protocol.

| <b>Tcirc:Trad</b> | <b>P Value</b> | <b>Significance</b> |
|-------------------|----------------|---------------------|
| Mounting          | 0.96           | n.s.                |
| 1:1               | 0.92           | n.s.                |
| 1:0.25            | 0.85           | n.s.                |
| 0.25:1            | 0.96           | n.s.                |

A colormap was generated to demonstrate the  $\theta_{\text{Fiber}}$  and DOA in different regions of the tissue under the four loading ratios for both pre-treatment and post-treatment (Figure 5-21). White lines indicate the average  $\theta_{\text{Fiber}}$  angle for the collagen fibers in the area. The colors represent the DOA, with cooler colors corresponding to higher DOA and less fiber alignment, and warmer colors corresponding to lower DOA and higher fiber alignment.



**Figure 5-21.** Colormap of leaflet before treatment and after treatment under four different loading ratios. White lines represent the average  $\theta_{\text{Fiber}}$  angle of collagen fibers in the area. Colors represent the DOA.

## 5.4 Discussion

The lack of statistically significant results from pre-treatment to post-treatment for the high tension and low-tension moduli in both the circumferential and radial directions is strong evidence suggesting that the chosen decellularization procedure maintains the mechanical properties of the native valve. Additionally, the control post-treatment to decellularized post-treatment comparison for the high tension and low-tension moduli in both circumferential and radial directions showed no statistically significant results, suggesting that the decellularization reagents do not cause further damage to the microstructure when compared to the DI water and PBS.

There was a general trend of increased peak stretch post-treatment compared to pre-treatment in both the circumferential and radial directions, however since this observation was made for both the control and the decellularized groups, this observation is most likely due to the tissues soaking in solution rather than the decellularization treatment itself.

A one-way MANOVA was implemented to investigate the effects of the treatment (decellularized vs. control) on several parameters including circumferential high-tension modulus, radial high-tension modulus, circumferential low tension modulus, radial low-tension modulus, circumferential peak stretch, and radial peak stretch. This MANOVA was repeated for each loading variable, and no statistically significant results were found for any of the loading conditions. These results suggest the decellularization treatment does not significantly affect any of the measured parameters when compared to the control treatment.

No statistically significant results were seen from pre-treatment to post-treatment for either the control group or the decellularized group, both for  $\theta_{\text{Fiber}}$  and DOA values. Additionally, control post-treatment to decellularized post-treatment tests showed no statistically significant

results for either  $\theta_{\text{Fiber}}$  or DOA. A one-way MANOVA was applied to this data as well, with the independent variable of treatment (decellularized vs. control) and dependent variables  $\theta_{\text{Fiber}}$  and DOA. This MANOVA was repeated for each loading ratio, and there were no statistically significant results observed. From this data, we can conclude that the decellularization treatment does not impact the collagen architecture of the leaflet.

# Chapter 6 Conclusions

## 6.1 Conclusions and Future Work

The optimized decellularization procedure chosen in this thesis (24 h detergents, 12 h enzymes) demonstrated lack of visible nuclei for all three leaflets with a sample size of 3 for each leaflet. Overall, the results from the biaxial testing resoundingly suggested that the chosen decellularization procedure effectively preserves the tissue mechanical properties of the native leaflet. However, due to time constraints, only a sample size of 5 was achieved. More testing should be done to confirm the results reported in this study.

While this study focused solely on leaflet tissue, future studies should be done to attempt decellularization of the whole valve, as this may be what is implanted into patients in the future. Once whole-valve decellularization is accomplished, the graft can be recellularized either in situ or in vitro with cells such as valvular interstitial cells, valvular endothelial cells, mesenchymal stem cells, and others. In addition to recellularization studies, the biaxial/pSFDI analysis – decellularization – biaxial/pSFDI analysis pipeline may be implemented with other tissues undergoing a tissue engineering study.

While more studies undoubtedly need to be done to confirm the findings in this thesis, these results provide an exciting first step toward a tissue-engineered heart valve that is hemocompatible, immunologically compatible, and readily remodeled to grow and adapt with the body.

1. Feldman, A. T. & Wolfe, D. Tissue Processing and Hematoxylin and Eosin Staining. in *Histopathology* (ed. Day, C. E.) vol. 1180 31–43 (Springer New York, 2014).
2. Basic Anatomy of the Human Heart. *Cardiology Associates of Michigan - Michigan's Best Heart Doctors* <https://www.cardofmich.com/anatomy-human-heart-fun-facts/> (2019).
3. Misfeld, M. & Sievers, H.-H. Heart valve macro- and microstructure. *Philos. Trans. R. Soc. B Biol. Sci.* **362**, 1421–1436 (2007).
4. Kramer, K. E. *et al.* An investigation of layer-specific tissue biomechanics of porcine atrioventricular valve anterior leaflets. *Acta Biomater.* **96**, 368–384 (2019).
5. Shah, P. M. & Raney, A. A. Tricuspid Valve Disease. *Curr. Probl. Cardiol.* **33**, 47–84 (2008).
6. Attenhofer Jost, C. H., Connolly, H. M., Dearani, J. A., Edwards, W. D. & Danielson, G. K. Ebstein's Anomaly. *Circulation* **115**, 277–285 (2007).
7. Rodés-Cabau, J., Taramasso, M. & O'Gara, P. T. Diagnosis and treatment of tricuspid valve disease: current and future perspectives. *The Lancet* **388**, 2431–2442 (2016).
8. Beckhoff, F. *et al.* Tricuspid Regurgitation – Medical Management and Evolving Interventional Concepts. *Front. Cardiovasc. Med.* **5**, 49 (2018).
9. Waller, B. F., Howard, J. & Fess, S. Pathology of tricuspid valve stenosis and pure tricuspid regurgitation-Part I. *Clin. Cardiol.* **18**, 97–102 (1995).
10. Marijon, E., Mirabel, M., Celermajer, D. S. & Jouven, X. Rheumatic heart disease. *The Lancet* **379**, 953–964 (2012).
11. Belluschi, I. *et al.* Surgical Techniques for Tricuspid Valve Disease. *Front. Cardiovasc. Med.* **5**, 118 (2018).
12. Yacoub, M. H. & Takkenberg, J. J. M. Will heart valve tissue engineering change the world? *Nat. Clin. Pract. Cardiovasc. Med.* **2**, 60–61 (2005).

13. VeDepo, M. C., Detamore, M. S., Hopkins, R. A. & Converse, G. L. Recellularization of decellularized heart valves: Progress toward the tissue-engineered heart valve. *J. Tissue Eng.* **8**, 204173141772632 (2017).
14. Argento, G., Simonet, M., Oomens, C. W. J. & Baaijens, F. P. T. Multi-scale mechanical characterization of scaffolds for heart valve tissue engineering. *J. Biomech.* **45**, 2893–2898 (2012).
15. Iop, L. *et al.* The influence of heart valve leaflet matrix characteristics on the interaction between human mesenchymal stem cells and decellularized scaffolds. *Biomaterials* **30**, 4104–4116 (2009).
16. Badylak, S. F. & Gilbert, T. W. Immune response to biologic scaffold materials. *Semin. Immunol.* **20**, 109–116 (2008).
17. Cooper, D. K. C., Ekser, B. & Tector, A. J. A brief history of clinical xenotransplantation. *Int. J. Surg.* **23**, 205–210 (2015).
18. Cooper, D. K. C., Ekser, B. & Tector, A. J. Immunobiological barriers to xenotransplantation. *Int. J. Surg.* **23**, 211–216 (2015).
19. Shimizu, A. *et al.* Acute Humoral Xenograft Rejection: Destruction of the Microvascular Capillary Endothelium in Pig-to-Nonhuman Primate Renal Grafts. *Lab. Invest.* **80**, 815–830 (2000).
20. Gilbert, T. W., Freund, J. M. & Badylak, S. F. Quantification of DNA in Biologic Scaffold Materials. *J. Surg. Res.* **152**, 135–139 (2009).
21. Valentin, J. E., Badylak, J. S., McCabe, G. P. & Badylak, S. F. Extracellular Matrix Bioscaffolds for Orthopaedic Applications. *VO L U M E* 14.

22. Badylak, S. F., Valentin, J. E., Ravindra, A. K., McCabe, G. P. & Stewart-Akers, A. M. Macrophage Phenotype as a Determinant of Biologic Scaffold Remodeling. *Tissue Eng. Part A* **14**, 1835–1842 (2008).
23. Valentin, J. E., Stewart-Akers, A. M., Gilbert, T. W. & Badylak, S. F. Macrophage Participation in the Degradation and Remodeling of Extracellular Matrix Scaffolds. *Tissue Eng. Part A* **15**, 1687–1694 (2009).
24. Fallon, A. M., Goodchild, T. T., Cox, J. L. & Matheny, R. G. In vivo remodeling potential of a novel bioprosthetic tricuspid valve in an ovine model. *J. Thorac. Cardiovasc. Surg.* **148**, 333-340.e1 (2014).
25. Reing, J. E. *et al.* Degradation Products of Extracellular Matrix Affect Cell Migration and Proliferation. *Tissue Eng. Part A* **15**, 605–614 (2009).
26. Larson, K., Ho, H. H., Anumolu, P. L. & Chen, M. T. Hematoxylin and Eosin Tissue Stain in Mohs Micrographic Surgery: A Review. *Dermatol. Surg.* **37**, 1089–1099 (2011).
27. Sampias, C., Ct, J. & Rolls, G. H&E Staining Overview: A Guide to Best Practices. *Best Pract.* **29**.
28. Rieder, E. *et al.* Tissue Engineering of Heart Valves: Decellularized Porcine and Human Valve Scaffolds Differ Importantly in Residual Potential to Attract Monocytic Cells. *Circulation* **111**, 2792–2797 (2005).
29. Dettin, M. *et al.* Natural Scaffolds for Regenerative Medicine: Direct Determination of Detergents Entrapped in Decellularized Heart Valves. *BioMed Res. Int.* **2017**, 1–9 (2017).
30. Cigliano, A. *et al.* Fine Structure of Glycosaminoglycans from Fresh and Decellularized Porcine Cardiac Valves and Pericardium. *Biochem. Res. Int.* **2012**, 1–10 (2012).



31. Kasimir, M.-T. *et al.* Comparison of Different Decellularization Procedures of Porcine Heart Valves. *Int. J. Artif. Organs* **26**, 421–427 (2003).
32. Yu, B.-T., Li, W.-T., Song, B.-Q. & Wu, Y.-L. Comparative study of the Triton X-100-sodium deoxycholate method and detergent-enzymatic digestion method for decellularization of porcine aortic valves. *Eur. Rev. Med. Pharmacol. Sci.* **17**, 2179–2184 (2013).
33. Meador, W. D. *et al.* A detailed mechanical and microstructural analysis of ovine tricuspid valve leaflets. *Acta Biomater.* **102**, 100–113 (2020).
34. Jett, S. V. *et al.* Integration of polarized spatial frequency domain imaging (pSFDI) with a biaxial mechanical testing system for quantification of load-dependent collagen architecture in soft collagenous tissues. *Acta Biomater.* **102**, 149–168 (2020).